Networks and Heterogeneous Media

https://www.aimspress.com/journal/nhm

NHM, 21(2): 496–530.
DOI: 10.3934/nhm.2026023
Received: 21 November 2025
Revised: 03 March 2026
Accepted: 17 March 2026
Published: 30 March 2026

Research article

Novel tick-borne encephalitis transmission dynamics: A model-based strategy for epidemic control

Zakirullah[1,*], Shakir Ullah[2], M. Motawi Khashan[3], Kamal Shah[2,4] and Thabet Abdeljawad[4,5,6,7,*]

[1] School of Mathematical Sciences, University of Electronic Science and Technology of China, Chengdu 611731, China

[2] Department of Mathematics, University of Malakand, Chakdara Dir(L), Khyber Pakhtunkhwa 18000, Pakistan

[3] Department of Basic Sciences, Common First Year, King Saud University, Riyadh 11451, Saudi Arabia

[4] Department of Mathematics and Sciences, Prince Sultan University, Riyadh 11586, Saudi Arabia

[5] Department of Fundamental Sciences, Faculty of Engineering and Architecture, Istanbul Gelisim University, Avcilar, Istanbul 34310, Turkey

[6] Department of Medical Research, China Medical University, Taichung 40402, Taiwan

[7] Department of Mathematics and Applied Mathematics School of Science and Technology, Sefako Makgatho Health Sciences University, Ga-Rankuwa, South Africa

* **Correspondence:** Email: zakirullahbzt@gmail.com, tabdeljawad@psu.edu.sa.

Abstract: This study, we present a fractional-order compartmental model to describe the transmission dynamics of tick-borne encephalitis between human and vector (tick) populations. The model is first formulated in the classical integer-order sense and then extended to a fractional-order framework using the Caputo fractional derivative to incorporate memory effects. We analyzed the model with respect to positivity, boundedness, and stability, and identified the invariant region under the Caputo fractional operator. Furthermore, the model was fitted to the reported case data, and $\mathcal{R}_0$ was computed using the next-generation matrix method, resulting in $\mathcal{R}_0 = 0.23$. PRCC sensitivity analysis confirmed the effectiveness of vaccination in reducing disease transmission, with local and global stability established through Jacobian and Lyapunov analyses, respectively. We examined the effect of the fractional-order parameter ζ using an efficient Adams-Moulton numerical approach, and contour and 3D surface plots are used to visualize the outcomes. The simulations showed that variations in key parameters reduced disease transmission and infection levels in both populations.

Keywords: tick-borne encephalitis; fractional-order mathematical model; stability analysis; Adams–Moulton method; parameter estimation

1. Introduction

Tick-borne encephalitis (TBE) is an emerging vector-borne viral infection caused by the tick-borne encephalitis virus (TBEV), and the virus is transmitted mainly through the bite of infected ticks, which acquire the virus while feeding on infected animal hosts and subsequently pass it to humans during blood meals. Following infection, the virus may invade the central nervous system, resulting in serious neurological disorders. Lindquist et al. [1], no effective antiviral treatment currently exists for tick-borne encephalitis virus (TBEV), making vaccination the primary preventive strategy, while Holding et al. [2] elucidated the viral structure and its neutralization by a monoclonal antibody, highlighting challenges for targeted therapy development. TBEV is a member of the *Flavivirus* genus within the *Flaviviridae* family. Moreover, an approximately 11 kb single-stranded RNA genome is possessed by the TBEV virus, which encodes the viral proteins required for replication, structural assembly, and successful infection of host cells [3]. The virus persists endemically across large regions, where it is continuously maintained within natural transmission cycles involving vectors and hosts of Europe and Asia, with reported circulation in at least 27 European countries and several Asian regions. Each year, approximately 10,000–12,000 human infections with tick-borne TBEV are reported worldwide, representing a significant public health burden across ecological and geographic regions, as reported by the World Health Organization. The epidemiology, ecological drivers, and prevention of TBEV have been discussed by Hotez et al. [4] and Süss [5]. Furthermore, WHO position papers [6] and the regional review by Xing et al. [7] emphasize vaccination strategies and disease dynamics in Europe and Asia, with particular attention to endemic regions in China. Since 2012, health authorities have classified TBE as a notifiable disease, requiring mandatory reporting to public health surveillance systems to enable timely monitoring and control of outbreaks in the European Union, and is subject to systematic surveillance [8]. In addition, researchers are actively conducting ongoing tick-monitoring programs across Europe, the United States, and the Netherlands, which continue to detect TBEV and other tick-borne viruses, highlighting the persistent and expanding risk posed by tick-borne pathogens, as reported by Jahfari et al. [9] and by Mansfield et al. [10]. Moreover, and recent systematic reviews by Qin et al. [11] further confirm the prevalence of TBEV in ticks and humans in China from 2000 to 2023.

Within China, TBE is classified as an occupational illness arising from biological exposure and is listed in the national occupational disease framework. However, the health authorities have not designated it as a nationally reportable infectious disease, which limits systematic monitoring and reporting of TBEV cases [12]. Currently, public health authorities in Heilongjiang Province are the only ones requiring mandatory reporting of TBE cases. However, researchers have not yet fully characterized the true magnitude of its impact on public health. Because surveillance is limited and underdiagnosis is possible, public health authorities may underestimate the true burden of TBEV infection; the number of infections is believed to exceed officially reported figures. Moreover, investigations conducted locally have revealed developments similar to those recorded in other European and Asian regions; the incidence of TBE in China has shown a persistent upward trajectory in recent years [13], and incidence of TBE in mainland China has increased in recent years. Researchers have yet to fully investigate the virus's transmission dynamics and associated risk factors. Furthermore, Effective vaccination is essential to preventing disease-related morbidity and mortality due to limited options for treating TBE. Three distinct pharmaceutical companies

presently hold licenses for five vaccine types in Europe and Russia: The vaccines produced by GSK-Encepur (Germany), Pfizer (Austria), Microgen (Russia), and the Chumakov Institute (licensed only within Russia) [14]. Individuals living in or traveling to endemic regions with a high risk of infection are strongly recommended to receive vaccination, which is widely recognized as the cornerstone of prevention, as highlighted by Zakirullah [15] and further supported by mathematical modeling studies on vaccination interventions by Zakirullah [16]. Researchers have also built a mathematical model to investigate this effect. The changing epidemiological landscape of TBE represents a growing public health challenge across the Eurasian region, highlighting the need for comprehensive analyses to clarify disease patterns and inform targeted prevention and control strategies for tick-borne viral infections in China [17].

Fractional-order modeling provides powerful tools for capturing memory effects in complex systems, as demonstrated by Du et al. [18] and by Naik et al. [19]. The application of artificial intelligence combined with fractional-order operators has enhanced data analysis in biomedical studies, as shown by Khan et al. [20]. Additionally, fractional frameworks are increasingly used to study transmission dynamics, control mechanisms, and complex systems, as highlighted by Devi et al. [21] and by Akgül et al. [22], with further insights into bifurcations and stability in cancer modeling provided by Xuan et al. [23]. Additionally, mathematical modeling approaches have provided additional insights into complex dynamics in related systems, as shown by Lu et al. [24]. In epidemiological models, fractional-order formulations have been shown to provide greater flexibility and improved agreement with observed data by capturing nonlocal temporal dynamics that are not effectively represented by classical integer-order models. As a result, fractional-order approaches have been increasingly applied to infectious disease modeling to better describe complex transmission processes and long-term system behavior. Fractional-order epidemic models have been used to study complex disease dynamics, including HIV/HCV co-infection, as demonstrated by Naik et al. [25] and Alkhazzan et al. [26]. Similarly, the dynamics of emerging infections such as monkeypox and Zika virus have been analyzed using fractional differential equations and AI-based modeling approaches by Khan et al. [27]. Furthermore, bifurcation and theoretical analyses have been applied to understand Hepatitis B and Ebola virus epidemics, as illustrated by Ahmad et al. [28] and Naik et al. [29].

Researchers studies have primarily relied on deterministic, integer-order eco-epidemiological models, which have been instrumental in advancing the understanding of TBE transmission dynamics [30]. Early studies focused on core transmission mechanisms and persistence thresholds, including non-viraemic transmission and host-vector interactions, as discussed by Mansfield et al. [31] and emphasized in recent reports by the WHO [32]. Additionally, researchers have studies on core transmission mechanisms and persistence thresholds, including non-viraemic transmission and host-vector interactions, as illustrated by Vorou et al. [33] and Kaiser et al. [34]. Subsequent models incorporated greater ecological realism by accounting for tick life stages, host structure, and spatial dynamics, highlighting the complexity of TBEV epidemiology. These modeling efforts provide essential insights for understanding transmission patterns and informing targeted control strategies. More recent work has highlighted the role of environmental variability and climate in shaping TBE risk and has emphasized data-driven calibration and scenario-based analyses to assess disease control strategies, as illustrated by Mittova et al. [35] and Süss [36]. Motivated by these gaps, compared with traditional models, we develop a new fractional-order human-vector transmission model for TBE that extends the classical integer-order framework by incorporating vaccination, hospitalization, and vector

dynamics within a unified Caputo fractional derivative setting. The proposed formulation captures memory-dependent effects in human and vector populations, enabling a more realistic representation of disease persistence and control.

The manuscript is organized as follows. In Section 2, we presents the essential preliminaries on fractional derivatives. The formulation of the TBE model, together with parameter descriptions and parameter estimation, is introduced in Section 3, where the integer-order and fractional-order frameworks are developed. The well-posedness of the proposed model is examined in Section 4. Section 5 is devoted to the derivation of equilibrium points, associated matrices, and the basic reproduction number $\mathcal{R}_0$. A comprehensive stability analysis is carried out in Section 6, followed by a sensitivity analysis in Section 7. The numerical scheme employed to solve the model is described in Section 8, while the corresponding numerical simulations and their interpretations are presented in Section 9. Finally, in Section 10, we summarize the major conclusions and key findings of the study.

2. Fractional calculus definitions

Key definitions of fractional derivatives are provided here.

Definition 2.1. *[37] Let $g : (0,\infty) \to \mathbb{R}$ be a real-valued function. The Riemann–Liouville fractional integral operator of order $\xi > 0$ is defined by*

$$ {}^{\mathrm{RL}}_{0}\mathcal{I}^{\xi}_{t} g(t) = \frac{1}{\Gamma(\xi)} \int_0^t (t-\psi)^{\xi-1} g(\psi)\, d\psi. $$

Definition 2.2. *[37] Let $g : (0,\infty) \to \mathbb{R}$ be a function and let $\xi > 0$ be the fractional order. The Riemann–Liouville fractional derivative of order ξ is defined by*

$$ {}^{\mathrm{RL}}_{0}\mathcal{D}^{\xi}_{t} g(t) = \begin{cases} \dfrac{1}{\Gamma(m-\xi)} \dfrac{d^m}{dt^m} \displaystyle\int_0^t (t-\psi)^{m-\xi-1} g(\psi)\, d\psi, & m-1 < \xi < m, \\ \dfrac{d^m}{dt^m} g(t), & \xi = m, \quad m \in \mathbb{N}. \end{cases} $$

Definition 2.3. *[38] Let $g(t)$ be a sufficiently smooth function and let $\xi > 0$ be a fractional order. The Laplace transform of the Caputo fractional derivative of order ξ is given by*

$$ \mathcal{L}\left[{}^{\mathrm{C}}_{0}D^{\xi}_{t} g(t) \right] = s^{\xi} G(s) - \sum_{k=0}^{m-1} g^{(k)}(0)\, s^{\xi-k-1}, $$

where $G(s) = \mathcal{L}[g(t)]$ and $m \in \mathbb{N}$ satisfies $m-1 < \xi \le m$.

Definition 2.4. *[39] The function $E_{m,n}(z)$, called the two-parameter Mittag–Leffler function, is defined by*

$$ E_{m,n}(z) = \sum_{k=0}^{\infty} \frac{z^k}{\Gamma(mk+n)}, \qquad m > 0,\ n > 0. $$

Moreover, its Laplace transform is given by

$$ \mathcal{L}\left[t^{n-1} E_{m,n}(\pm a t^m) \right](s) = \frac{s^{m-n}}{s^m \mp a}. $$

Lemma 2.4.1. *[39] Consider the fractional differential equation*

$$^{C}\mathcal{D}_{t}^{\xi}\Upsilon(t) = C(\Upsilon(t)), \qquad \Upsilon(t_0) = (y_1(t_0), y_2(t_0), \ldots, y_n(t_0)),$$

where $0 < \xi < 1$, $\Upsilon(t) = (y_1(t), y_2(t), \ldots, y_n(t)) \in \mathbb{R}^n$ *is the state vector, and*

$$C : \mathbb{R}^n \to \mathbb{R}^n$$

is a continuous vector field describing the system dynamics.

Lemma 2.4.2. *[39] Let* $y(t) \in \mathbb{R}_+$ *be a differentiable function. Then, for all* $t > 0$ *and* $\xi \in (0, 1)$*, the following inequality holds:*

$$^{C}\mathcal{D}_{t}^{\xi}y(t) \leq y^* - y^* \ln\left(\frac{y(t)}{y^*}\right) - \left(1 - \frac{y^*}{y(t)}\right)^{C}\mathcal{D}_{t}^{\xi}y(t), \qquad y^* \in \mathbb{R}_+.$$

3. Model development

In this section, a compartmental model is proposed to describe the transmission dynamics of TBE between human and vector (tick) populations. The human population is divided into six compartments: susceptible (S_h), vaccinated (V_h), exposed (E_h), infectious (I_h), hospitalized (H_h), and recovered (R_h). The vector population is classified into three compartments: susceptible (S_v), exposed (E_v), and infectious (I_v).

In the susceptible human class S_h, τ_h denotes the human recruitment rate, a is the vector biting rate, b is the transmission probability from vector to human, I_v represents infectious vectors, d_h is the natural death rate of humans, and ν is the vaccination rate:

$$\frac{dS_h}{dt} = \tau_h - (abI_v + d_h + \nu)S_h.$$

In the vaccinated human class V_h, ν is the vaccination rate, S_h is the susceptible human population, and d_h denotes the natural death rate:

$$\frac{dV_h}{dt} = \nu S_h - d_h V_h.$$

In the exposed human class E_h, a is the biting rate, b is the transmission probability, I_v denotes infectious vectors, η_1 and σ are progression and subclinical recovery rates, respectively, and d_h is the natural death rate:

$$\frac{dE_h}{dt} = abI_v S_h - (\eta_1 + \sigma + d_h)E_h.$$

In the infectious human class I_h, η_1 is the progression rate from exposed to infectious, θ is the recovery rate, δ is the hospitalization rate, and d_h is the natural death rate:

$$\frac{dI_h}{dt} = \eta_1 E_h - (\theta + \delta + d_h)I_h.$$

In the hospitalized human class H_h, δ denotes the hospitalization rate, γ is the recovery rate of hospitalized individuals, and d_h is the natural death rate:

$$\frac{dH_h}{dt} = \delta I_h - (\gamma + d_h)H_h.$$

In the recovered human class R_h, σ, θ, and γ represent recovery rates from exposed, infectious, and hospitalized classes, respectively, while d_h is the natural death rate:

$$\frac{dR_h}{dt} = \sigma E_h + \theta I_h + \gamma H_h - d_h R_h.$$

In the susceptible vector class S_v, τ_v is the vector recruitment rate, a is the biting rate, c is the transmission probability from human to vector, I_h is the infectious human population, and d_v is the natural vector death rate:

$$\frac{dS_v}{dt} = \tau_v - (acI_h + d_v)S_v.$$

In the exposed vector class E_v, a is the biting rate, c is the transmission probability, η_2 is the progression rate in vectors, and d_v is the natural death rate:

$$\frac{dE_v}{dt} = acI_h S_v - (d_v + \eta_2)E_v.$$

In the infectious vector class I_v, η_2 is the progression rate to infectious vectors, ξ denotes the disease-induced vector death rate, and d_v is the natural death rate:

$$\frac{dI_v}{dt} = \eta_2 E_v - (\xi + d_v)I_v. \tag{3.1}$$

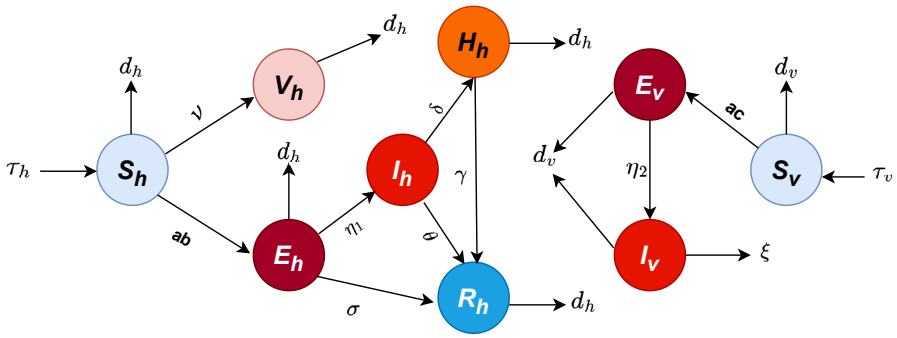

Figure 1. Schematic diagram representing the epidemic dynamics of tick-borne encephalitis.

Using the integer-order model as a baseline, and flow diagram in Figure 1, the model is reformulated in the Caputo fractional-order sense as follows:

$$\begin{aligned}
{}^{\mathscr{C}}\mathscr{D}_t^{\zeta} S_h &= \tau_h - (abI_v + d_h + \nu)S_h,\\
{}^{\mathscr{C}}\mathscr{D}_t^{\zeta} V_h &= \nu S_h - d_h V_h,\\
{}^{\mathscr{C}}\mathscr{D}_t^{\zeta} E_h &= abI_v S_h - (\eta_1 + \sigma + d_h)E_h,\\
{}^{\mathscr{C}}\mathscr{D}_t^{\zeta} I_h &= \eta_1 E_h - (\theta + \delta + d_h)I_h,\\
{}^{\mathscr{C}}\mathscr{D}_t^{\zeta} H_h &= \delta I_h - (\gamma + d_h)H_h,\\
{}^{\mathscr{C}}\mathscr{D}_t^{\zeta} R_h &= \sigma E_h + \theta I_h + \gamma H_h - d_h R_h,\\
{}^{\mathscr{C}}\mathscr{D}_t^{\zeta} S_v &= \tau_v - (acI_h + d_v)S_v,
\end{aligned}$$

$$
\begin{aligned}
{}^{\mathscr{C}}\mathscr{D}_t^{\zeta} E_v &= acI_h S_v - (d_v + \eta_2)E_v, \\
{}^{\mathscr{C}}\mathscr{D}_t^{\zeta} I_v &= \eta_2 E_v - (\xi + d_v)I_v,
\end{aligned} \tag{3.2}
$$

subject to the initial conditions

$$
S_h, V_h, E_h, I_h, H_h, R_h, S_v, E_v, I_v \geq 0.
$$

3.1. Parameter estimation

In this subsection, model parameters are estimated using a nonlinear least-squares framework by minimizing the residuals between the simulated outputs and the reported TBE infection data. Figure 2(a) shows a close agreement between the model-predicted infection trajectory and the observed data, while the corresponding residuals are displayed in Figure 2(b).

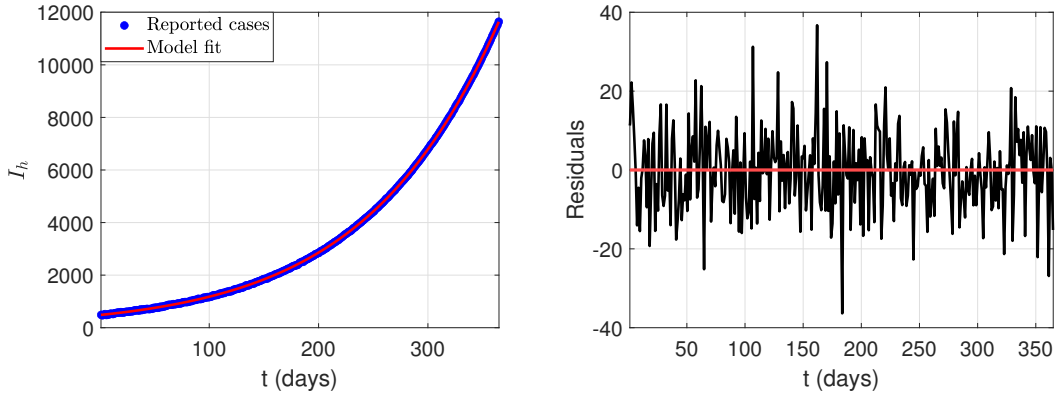

(a) **(b)**

Figure 2. Model fit to the reported TBE infection data.

Parameter estimation is performed using MATLAB's built-in `lsqcurvefit` routine, which implements nonlinear least-squares optimization. Model (3.2) involves fifteen parameters; some of these are fixed based on values available in the literature, whereas the remaining parameters are estimated using the reported TBE case data in [40].

To assess the goodness of fit, the root mean square error (RMSE) between the simulated infection data $\Upsilon(t_n)$ and the observed data $\Upsilon_{\text{data}}(t_n)$ is computed as

$$
\text{RMSE} = \sqrt{\frac{1}{l}\sum_{n=1}^{l} (\Upsilon(t_n) - \Upsilon_{\text{data}}(t_n))^2},
$$

where l denotes the total number of observation time points.

The proposed framework is the incorporation of a fractional-order derivative of order ζ, which increases model flexibility and enable the explicit representation of memory effects in disease transmission dynamics. Specifically, the evolution of the cumulative infected population $\chi(t)$ is governed by

$$
{}^{\mathscr{C}}\mathscr{D}_t^{\zeta}\chi(t) = \eta_1^{\zeta} E_h - (\theta^{\zeta} + \delta^{\zeta} + d_h^{\zeta})I_h,
$$

where the daily number of newly reported infections is defined as $\mathcal{Z}(t) = \chi(t) - \chi(t-1)$.

The optimal parameter set is obtained for $\zeta = 0.71$, indicating the presence of memory effects in TBE transmission. Consistent with this observation, the fractional-order model provides a noticeably improved fit to the reported data compared with its integer-order counterpart. The estimated parameter values corresponding to the best fit are summarized in Table 1.

Table 1. Descriptions of model parameter values and sensitivity indices.

Parameter	Description	Value (per day))	SI	Source
τ_h	Recruitment rate of humans	$537915 \times \frac{1}{365}$	+0.500	[41]
d_h	Natural death rate of humans	$\frac{1}{79 \times 365}$	−0.0003	[42]
ν	Vaccination rate of susceptible humans	0.090	−0.49	Fitted
a	Biting rate of vectors on humans	0.05–0.1	+1.000	Fitted
b	Vector-to-human transmission probability per bite	0.020	+0.500	Fitted
c	Human-to-vector transmission probability per bite	0.041	+0.500	Fitted
η_1	Exposed-to-infectious rate for humans	0.020	0.46	Fitted
σ	Rate of asymptomatic recovery in exposed humans	0.230	−0.456	Fitted
θ	Recovery rate of infectious humans	0.080	−0.165	Fitted
δ	Hospitalization rate of infectious humans	0.160	−0.330	Fitted
γ	Recovery rate of hospitalized humans	0.570	-	Fitted
τ_v	Recruitment rate of vectors	0.0027	0.5	[43]
d_v	Natural death rate of vectors	0.017	−0.91	[43]
η_2	Exposed-to-infectious rate for vectors	0.07	0.097	Fitted
ξ	Vector death rate	0.01	−0.18	Fitted

4. Non-negativity, boundedness, existence, and uniqueness

In this sectioned, we establishes the well-posedness of the model, including positivity, boundedness, exactness, and uniqueness of the solutions.

Proposition 4.1. *Let all model parameters be positive and suppose the initial conditions satisfy*

$$S_h(0), V_h(0), E_h(0), I_h(0), H_h(0), R_h(0), S_v(0), E_v(0), I_v(0) \geq 0.$$

Then, for every $t > 0$, system (3.2) *admits a solution that is non-negative, bounded, and trajectory remains in a positively invariant region*

$$\Omega = \Omega_h \times \Omega_v,$$

where

$$\Omega_h = \left\{ (S_h, V_h, E_h, I_h, H_h, R_h) \in R_+^6 : \mathcal{N}_h(t) = S_h + V_h + E_h + I_h + H_h + R_h \leq \frac{\tau_h}{d_h} \right\},$$

$$\Omega_v = \left\{ (S_v, E_v, I_v) \in R_+^3 : \mathcal{N}_v(t) = S_v + E_v + I_v \leq \frac{\tau_v}{d_v} \right\}.$$

Proposition 4.2. *To guarantee the non-negativity of the state variables, consider the fractional-order differential equation for the susceptible human population* $S_h(t)$

$$^{\mathscr{C}}\mathscr{D}_t^{\zeta} S_h = \tau_h - (b_1 b_2 I_v + \nu + d_h) S_h.$$

This takes the form:

$$^{\mathscr{C}}\mathscr{D}_t^{\zeta} S_h + (\nu + d_h) S_h = \tau_h \geq 0.$$

Since $\tau_h \geq 0$ the positivity of the Caputo derivative leads to $S_h(t) \geq 0$ for all $t > 0$.
Applying the Laplace transform, we obtain

$$s^{\zeta}\mathscr{L}[S_h] - s^{\zeta-1} S_h(0) + (\nu + d_h)\mathscr{L}[S_h] \geq 0,$$

$$\mathscr{L}[S_h] \geq \frac{s^{\zeta-1} S_h(0)}{s^{\zeta} + (\nu + d_h)}.$$

The inverse Laplace transform yields

$$S_h(t) \geq S_h(0) E_{\zeta,1}\left(-(\nu + d_h) t^{\zeta}\right) \geq 0.$$

Similarly, all remaining variables $V_h, E_h, I_h, H_h, R_h, S_v, E_v, I_v$ follow a fractional differential equation structured as

$$^{\mathscr{C}}\mathscr{D}_t^{\zeta} x(t) + a(t) x(t) = f(t) \geq 0,$$

with the same approach, positivity for all compartments holds for $t > 0$. We proceed to show boundedness. Let the total human population be defined as

$$\mathscr{N}_h(t) = S_h(t) + V_h(t) + E_h(t) + I_h(t) + H_h(t) + R_h(t).$$

The sum of the equations gives

$$^{\mathscr{C}}\mathscr{D}_t^{\zeta} \mathscr{N}_h(t) = \tau_h - d_h \mathscr{N}_h(t).$$

We consider the Laplace transform of this linear fractional differential equation

$$s^{\zeta}\mathscr{L}[\mathscr{N}_h] - s^{\zeta-1}\mathscr{N}_h(0) = \frac{\tau_h}{s} - d_h \mathscr{L}[\mathscr{N}_h],$$

$$\mathscr{L}[\mathscr{N}_h] = \frac{s^{\zeta-1}\mathscr{N}_h(0) + \tau_h/s}{s^{\zeta} + d_h}.$$

By taking the inverse Laplace transform, we get

$$\mathscr{N}_h(t) = \mathscr{N}_h(0) E_{\zeta,1}\left(-d_h t^{\zeta}\right) + \tau_h E_{\zeta,\zeta+1}(-d_h t^{\zeta}).$$

Following the Mittag-Leffler function, we get

$$E_{c,d}(x) = x E_{c,c+d}(x) + \frac{1}{\Gamma(d)}.$$

Hence,

$$\mathscr{N}_h(t) = (\mathscr{N}_h(0) - \frac{\tau_h}{d_h})E_{\zeta,1}(-d_h t^{\zeta}) + \frac{\tau_h}{d_h}.$$

Thus, $\lim_{t\to\infty} \sup N(t) \leq \frac{\tau_h}{d_h}$.
As a result, $\mathscr{N}_h(t)$ is bounded.
The same approach is applied to the vector population

$$^{\mathscr{C}}\mathscr{D}_t^{\zeta}\mathscr{N}_v(t) = \zeta_v - d_v\mathscr{N}_v(t) \Rightarrow \mathscr{N}_v(t) \leq \frac{\tau_v}{d_v}.$$

As a result, all system variables are non-negative and bounded, which confirms the positive invariance and epidemiological feasibility of the region $\Omega \subset R_+^9$.

4.1. Existence and uniqueness

In this subsection, we present the conditions that ensure existence and uniqueness proofs for the solution of the fractional-order system (3.2).

Theorem 4.1. *Let the initial condition be given in a bounded region* $\mathscr{K} \times (0, T]$*, where*

$$\mathscr{K} = \left\{(S_h, V_h, E_h, I_h, H_h, R_h, S_v, E_v, I_v) \in R^9 : \max\{|S_h|, |V_h|, |E_h|, |I_h|, |H_h|, |R_h|, |S_v|, |E_v|, |I_v|\} \leq M\right\}.$$

The fractional-order system (3.2) *has a unique solution for each initial condition in* $\mathscr{K}$ *.*

Proof. Let us define the mapping

$$\mathscr{F}(\mathscr{Y}) = (\mathscr{F}_1(\mathscr{Y}), \mathscr{F}_2(\mathscr{Y}), \ldots, \mathscr{F}_9(\mathscr{Y})),$$

where $\mathscr{Y} = (S_h, V_h, E_h, I_h, H_h, R_h, S_v, E_v, I_v)$, and the components of $\mathscr{F}(\mathscr{Y})$ are given by

$$\begin{aligned}
\mathscr{F}_1(\mathscr{Y}) &= \tau_h - abI_vS_h - (d_h + \nu)S_h,\\
\mathscr{F}_2(\mathscr{Y}) &= \nu S_h - d_hV_h,\\
\mathscr{F}_3(\mathscr{Y}) &= abI_vS_h - (\eta_1 + \sigma + d_h)E_h,\\
\mathscr{F}_4(\mathscr{Y}) &= \eta_1E_h - (\theta + \delta + d_h)I_h,\\
\mathscr{F}_5(\mathscr{Y}) &= \delta I_h - (\gamma + d_h)H_h,\\
\mathscr{F}_6(\mathscr{Y}) &= \sigma E_h + \theta I_h + \gamma H_h - d_hR_h,\\
\mathscr{F}_7(\mathscr{Y}) &= \tau_v - acI_hS_v - d_vS_v,\\
\mathscr{F}_8(\mathscr{Y}) &= acI_hS_v - (d_v + \eta_2)E_v,\\
\mathscr{F}_9(\mathscr{Y}) &= \eta_2E_v - d_vI_v.
\end{aligned}$$

To prove the Lipschitz condition, consider any $\mathscr{Y}, \widetilde{\mathscr{Y}} \in \mathscr{K}$. Then

$$\begin{aligned}
\|\mathscr{F}(\mathscr{Y}) - \mathscr{F}(\widetilde{\mathscr{Y}})\| &\leq \sum_{i=1}^{9} |\mathscr{F}_i(\mathscr{Y}) - \mathscr{F}_i(\widetilde{\mathscr{Y}})|\\
&\leq G_1|S_h - \widetilde{S}_h| + G_2|V_h - \widetilde{V}_h| + G_3|E_h - \widetilde{E}_h| + G_4|I_h - \widetilde{I}_h| + G_5|H_h - \widetilde{H}_h|
\end{aligned}$$

$$+ G_6|R_h - \widetilde{R}_h| + G_7|S_v - \widetilde{S}_v| + G_8|E_v - \widetilde{E}_v| + G_9|I_v - \widetilde{I}_v|.$$

It follows that there exists a constant $G > 0$ satisfying:

$$\|\mathscr{F}(\mathscr{Y}) - \mathscr{F}(\widetilde{\mathscr{Y}})\| \leq G\|\mathscr{Y} - \widetilde{\mathscr{Y}}\|.$$

This proves that $\mathscr{F}$ is Lipschitz continuous on $\mathscr{K}$. Consequently, given Theorem 4.1, for fractional differential equations with Lipschitz nonlinearity, system (3.2) admits a unique solution for each initial condition.

5. Equilibria and basic reproduction number ($\mathcal{R}_0$)

In this section, we derive the disease-free equilibrium (DFE), compute $\mathcal{R}_0$ using the next-generation matrix approach, and establish the endemic equilibrium (EE) of the model.

The DFE corresponds to the absence of infection in the population. Setting

$${}^{\mathscr{C}}\mathscr{D}_t^{\zeta} S_h = {}^{\mathscr{C}}\mathscr{D}_t^{\zeta} E_h = {}^{\mathscr{C}}\mathscr{D}_t^{\zeta} I_h = {}^{\mathscr{C}}\mathscr{D}_t^{\zeta} H_h = {}^{\mathscr{C}}\mathscr{D}_t^{\zeta} R_h = {}^{\mathscr{C}}\mathscr{D}_t^{\zeta} S_v = {}^{\mathscr{C}}\mathscr{D}_t^{\zeta} E_v = {}^{\mathscr{C}}\mathscr{D}_t^{\zeta} I_v = 0$$

and assuming that all infected compartments vanish, we obtain the disease-free equilibrium

$$E^0 = (S_h^0, V_h^0, E_h^0, I_h^0, H_h^0, R_h^0, S_v^0, E_v^0, I_v^0),$$

where

$$\begin{aligned} S_h^0 &= \frac{\tau_h}{d_h + \nu}, \\ V_h^0 &= \frac{\nu\tau_h}{d_h(d_h + \nu)}, \\ S_v^0 &= \frac{\tau_v}{d_v}. \end{aligned} \tag{5.1}$$

To compute the basic reproduction number $\mathcal{R}_0$, we apply the next-generation matrix method by considering the infected compartments E_h, I_h, E_v, and I_v. The dynamics of the infected classes are given by

$$\begin{aligned} {}^{\mathscr{C}}\mathscr{D}_t^{\zeta} E_h &= abI_v S_h - (\eta_1 + \sigma + d_h)E_h, \\ {}^{\mathscr{C}}\mathscr{D}_t^{\zeta} I_h &= \eta_1 E_h - (\theta + \delta + d_h)I_h, \\ {}^{\mathscr{C}}\mathscr{D}_t^{\zeta} E_v &= acI_h S_v - (d_v + \eta_2)E_v, \\ {}^{\mathscr{C}}\mathscr{D}_t^{\zeta} I_v &= \eta_2 E_v - (\xi + d_v)I_v. \end{aligned} \tag{5.2}$$

Let F denote the rate of new infections in the system, and let V represent the transfer of individuals into and out of the infected compartments. Based on system (5.2), we then define the following matrices:

$$F = \begin{pmatrix} abI_v S_h \\ 0 \\ acI_h S_v \\ 0 \end{pmatrix},$$

and

$$V = \begin{pmatrix} (\eta_1 + \sigma + d_h)E_h \\ -\eta_1 E_h + (\theta + \delta + d_h)I_h \\ (d_v + \eta_2)E_v \\ -\eta_2 E_v + (\xi + d_v)I_v \end{pmatrix}.$$

Let J_F and J_V denote the Jacobian matrices of F and V with respect to the infected variables (E_h, I_h, E_v, I_v). Defining

$$\begin{aligned} &\Delta_1 = abI_vS_h,\ \Delta_2 = 0,\ \Delta_3 = acI_hS_v,\ \Delta_4 = 0, \\ &\Lambda_1 = (\eta_1 + \sigma + d_h)E_h,\ \Lambda_2 = -\eta_1 E_h + (\theta + \delta + d_h)I_h, \\ &\Lambda_3 = (d_v + \eta_2)E_v,\ \Lambda_4 = -\eta_2 E_v + (\xi + d_v)I_v, \end{aligned}$$

we obtain

$$J_F = \begin{pmatrix} \frac{\partial\Delta_1}{\partial E_h} & \frac{\partial\Delta_1}{\partial I_h} & \frac{\partial\Delta_1}{\partial E_v} & \frac{\partial\Delta_1}{\partial I_v} \\ \frac{\partial\Delta_2}{\partial E_h} & \frac{\partial\Delta_2}{\partial I_h} & \frac{\partial\Delta_2}{\partial E_v} & \frac{\partial\Delta_2}{\partial I_v} \\ \frac{\partial\Delta_3}{\partial E_h} & \frac{\partial\Delta_3}{\partial I_h} & \frac{\partial\Delta_3}{\partial E_v} & \frac{\partial\Delta_3}{\partial I_v} \\ \frac{\partial\Delta_4}{\partial E_h} & \frac{\partial\Delta_4}{\partial I_h} & \frac{\partial\Delta_4}{\partial E_v} & \frac{\partial\Delta_4}{\partial I_v} \end{pmatrix} = \begin{pmatrix} 0 & 0 & 0 & abS_h \\ 0 & 0 & 0 & 0 \\ 0 & acS_v & 0 & 0 \\ 0 & 0 & 0 & 0 \end{pmatrix},$$

and

$$J_V = \begin{pmatrix} \frac{\partial\Lambda_1}{\partial E_h} & \frac{\partial\Lambda_1}{\partial I_h} & \frac{\partial\Lambda_1}{\partial E_v} & \frac{\partial\Lambda_1}{\partial I_v} \\ \frac{\partial\Lambda_2}{\partial E_h} & \frac{\partial\Lambda_2}{\partial I_h} & \frac{\partial\Lambda_2}{\partial E_v} & \frac{\partial\Lambda_2}{\partial I_v} \\ \frac{\partial\Lambda_3}{\partial E_h} & \frac{\partial\Lambda_3}{\partial I_h} & \frac{\partial\Lambda_3}{\partial E_v} & \frac{\partial\Lambda_3}{\partial I_v} \\ \frac{\partial\Lambda_4}{\partial E_h} & \frac{\partial\Lambda_4}{\partial I_h} & \frac{\partial\Lambda_4}{\partial E_v} & \frac{\partial\Lambda_4}{\partial I_v} \end{pmatrix} = \begin{pmatrix} \eta_1 + \sigma + d_h & 0 & 0 & 0 \\ -\eta_1 & \theta + \delta + d_h & 0 & 0 \\ 0 & 0 & d_v + \eta_2 & 0 \\ 0 & 0 & -\eta_2 & \xi + d_v \end{pmatrix}.$$

Evaluating these matrices at the disease-free equilibrium E^0, we obtain

$$J_F(E^0) = \begin{pmatrix} 0 & 0 & 0 & \frac{ab\tau_h}{d_h+\nu} \\ 0 & 0 & 0 & 0 \\ 0 & \frac{ac\tau_v}{d_v} & 0 & 0 \\ 0 & 0 & 0 & 0 \end{pmatrix}, \qquad J_V(E^0) = \begin{pmatrix} \eta_1 + \sigma + d_h & 0 & 0 & 0 \\ -\eta_1 & \theta + \delta + d_h & 0 & 0 \\ 0 & 0 & d_v + \eta_2 & 0 \\ 0 & 0 & -\eta_2 & \xi + d_v \end{pmatrix}.$$

The inverse of $J_V(E^0)$ is given by

$$J_V(E^0)^{-1} = \begin{pmatrix} \frac{1}{\sigma+\eta_1+d_h} & 0 & 0 & 0 \\ \frac{\eta_1}{(\sigma+\eta_1+d_h)(\theta+\delta+d_h)} & \frac{1}{\theta+\delta+d_h} & 0 & 0 \\ 0 & 0 & \frac{1}{\eta_2+d_v} & 0 \\ 0 & 0 & \frac{\eta_2}{(\xi+d_v)(\eta_2+d_v)} & \frac{1}{\xi+d_v} \end{pmatrix}.$$

Consequently, the next-generation matrix is

$$J_F(E^0)J_V(E^0)^{-1} = \begin{pmatrix} 0 & 0 & \frac{ab\eta_2\tau_h}{(\nu+d_h)(\xi+d_v)(\eta_2+d_v)} & \frac{ab\tau_h}{(\nu+d_h)(\xi+d_v)} \\ 0 & 0 & 0 & 0 \\ \frac{ac\eta_1\tau_v}{d_v(\sigma+\eta_1+d_h)(\theta+\delta+d_h)} & \frac{ac\tau_v}{d_v(\theta+\delta+d_h)} & 0 & 0 \\ 0 & 0 & 0 & 0 \end{pmatrix}.$$

The eigenvalues of $J_F(E^0)J_V(E^0)^{-1}$ are

$$\lambda_1 = \lambda_2 = 0,$$
$$\lambda_3 = -a\sqrt{\frac{bc\eta_1\eta_2\tau_h\tau_v}{d_v\,(\nu + d_h)\,(\xi + d_v)\,(\eta_2 + d_v)\,(\sigma + \eta_1 + d_h)\,(\theta + \delta + d_h)}},$$
$$\lambda_4 = a\sqrt{\frac{bc\eta_1\eta_2\tau_h\tau_v}{d_v\,(\nu + d_h)\,(\xi + d_v)\,(\eta_2 + d_v)\,(\sigma + \eta_1 + d_h)\,(\theta + \delta + d_h)}}.$$

The basic reproduction number, $\mathcal{R}_0$, is defined as the spectral radius, that is, the largest eigenvalue, of the matrix product $J_F(E^0)J_V(E^0)^{-1}$. Accordingly, we have

$$\mathcal{R}_0 = a\sqrt{\frac{bc\eta_1\eta_2\tau_h\tau_v}{d_v\,(\nu + d_h)\,(\xi + d_v)\,(\eta_2 + d_v)\,(\sigma + \eta_1 + d_h)\,(\theta + \delta + d_h)}}.$$

Next, the EE exists when the disease persists in the population; that is,

$$E_h^\star > 0, I_h^\star > 0, E_v^\star > 0, I_v^\star > 0.$$

To derive the EE, we assume all compartments are nonzero

$${}^{\mathscr{C}}\mathscr{D}_t^\zeta S_h \neq^{\mathscr{C}} \mathscr{D}_t^\zeta E_h \neq^{\mathscr{C}} \mathscr{D}_t^\zeta I_h \neq^{\mathscr{C}} \mathscr{D}_t^\zeta H_h \neq^{\mathscr{C}} \mathscr{D}_t^\zeta R_h \neq^{\mathscr{C}} \mathscr{D}_t^\zeta S_v \neq^{\mathscr{C}} \mathscr{D}_t^\zeta E_v \neq^{\mathscr{C}} \mathscr{D}_t^\zeta I_v \neq 0.$$

The endemic equilibrium $E^\star$ is obtained by setting all derivatives in system (3.2) to zero. Solving the resulting algebraic system yields the endemic equilibrium (EE), given by

$$E^\star = (S_h^\star, V_h^\star, E_h^\star, I_h^\star, H_h^\star, R_h^\star, S_v^\star, E_v^\star, I_v^\star),$$

where

$$\begin{aligned}
S_h^\star &= \frac{\xi + d_v\tau_h}{Z},\\
V_h^\star &= \frac{\tau_h\nu\xi + d_v}{d_hZ},\\
E_h^\star &= \frac{ab\tau_h(\tau_v - N_v)}{(\eta_1 + \sigma + d_h)Z},\\
I_h^\star &= \frac{ab\eta_1\tau_h(\tau_v - N_v)}{(\eta_1 + \sigma + d_h)\,(\theta + \delta + d_h)Z},\\
H_h^\star &= \frac{ab\eta_1\delta\tau_h(\tau_v - N_v)}{(\eta_1 + \sigma + d_h)\,(\theta + \delta + d_h)Z(\gamma + d_h)},\\
R_h^\star &= \frac{ab\sigma\tau_h(\tau_v - N_v)}{d_h(\eta_1 + \sigma + d_h)Z}(1 + \frac{\eta_1\,(\theta\gamma + \gamma\delta + \theta d_h)}{(\theta + \delta + d_h)\,(\gamma + d_h)}),\\
S_v^\star &= \frac{d_v\tau_v - (d_v + \eta_2)N_v}{d_v\eta_2},\\
E_v^\star &= \frac{\tau_v - N_v}{\eta_2},\\
I_v^\star &= \frac{\tau_v - N_v}{\xi + d_v},
\end{aligned}$$

with

$$Z = (\nu\xi + \xi d_h - \nu d_v - d_hd_v + ab\tau_v - abN_v)\,.$$

6. Local and global stability

This section, we present local and global stability analyses.

Theorem 6.1. *The DFE E^0 of system* (3.2) *remains locally asymptotically stable (LAS) under the condition $\mathcal{R}_0 < 1$, whereas it becomes unstable if $\mathcal{R}_0 > 1$.*

Proof. To establish the local stability of DFE, we consider the Jacobian matrix of system (3.2) evaluated at E_0. We define the nonlinear components as

$$\begin{aligned}
\Theta_1 &= \tau_h - (abI_v + d_h + \nu)S_h,\\
\Theta_2 &= \nu S_h - d_h V_h,\\
\Theta_3 &= abI_v S_h - (\eta_1 + \sigma + d_h)E_h,\\
\Theta_4 &= \eta_1 E_h - (\theta + \delta + d_h)I_h,\\
\Theta_5 &= \delta I_h - (\gamma + d_h)H_h,\\
\Theta_6 &= \sigma E_h + \theta I_h + \gamma H_h - d_h R_h,\\
\Theta_7 &= \tau_v - (acI_h + d_v)S_v,\\
\Theta_8 &= acI_h S_v - (d_v + \eta_2)E_v,\\
\Theta_9 &= \eta_2 E_v - (\xi + d_v)I_v.
\end{aligned}$$

The Jacobian matrix associated with the subsystem $(S_h, V_h, E_h, I_h, H_h, R_h, S_v, E_v, I_v)$ is given by

$$J(E) = \begin{pmatrix}
\frac{\partial\Theta_1}{\partial S_h} & \frac{\partial\Theta_1}{\partial V_h} & \frac{\partial\Theta_1}{\partial E_h} & \frac{\partial\Theta_1}{\partial I_h} & \frac{\partial\Theta_1}{\partial H_h} & \frac{\partial\Theta_1}{\partial R_h} & \frac{\partial\Theta_1}{\partial S_v} & \frac{\partial\Theta_1}{\partial E_v} & \frac{\partial\Theta_1}{\partial I_v}\\
\frac{\partial\Theta_2}{\partial S_h} & \frac{\partial\Theta_2}{\partial V_h} & \frac{\partial\Theta_2}{\partial E_h} & \frac{\partial\Theta_2}{\partial I_h} & \frac{\partial\Theta_2}{\partial H_h} & \frac{\partial\Theta_2}{\partial R_h} & \frac{\partial\Theta_2}{\partial S_v} & \frac{\partial\Theta_2}{\partial E_v} & \frac{\partial\Theta_2}{\partial I_v}\\
\frac{\partial\Theta_3}{\partial S_h} & \frac{\partial\Theta_3}{\partial V_h} & \frac{\partial\Theta_3}{\partial E_h} & \frac{\partial\Theta_3}{\partial I_h} & \frac{\partial\Theta_3}{\partial H_h} & \frac{\partial\Theta_3}{\partial R_h} & \frac{\partial\Theta_3}{\partial S_v} & \frac{\partial\Theta_3}{\partial E_v} & \frac{\partial\Theta_3}{\partial I_v}\\
\frac{\partial\Theta_4}{\partial S_h} & \frac{\partial\Theta_4}{\partial V_h} & \frac{\partial\Theta_4}{\partial E_h} & \frac{\partial\Theta_4}{\partial I_h} & \frac{\partial\Theta_4}{\partial H_h} & \frac{\partial\Theta_4}{\partial R_h} & \frac{\partial\Theta_4}{\partial S_v} & \frac{\partial\Theta_4}{\partial E_v} & \frac{\partial\Theta_4}{\partial I_v}\\
\frac{\partial\Theta_5}{\partial S_h} & \frac{\partial\Theta_5}{\partial V_h} & \frac{\partial\Theta_5}{\partial E_h} & \frac{\partial\Theta_5}{\partial I_h} & \frac{\partial\Theta_5}{\partial H_h} & \frac{\partial\Theta_5}{\partial R_h} & \frac{\partial\Theta_5}{\partial S_v} & \frac{\partial\Theta_5}{\partial E_v} & \frac{\partial\Theta_5}{\partial I_v}\\
\frac{\partial\Theta_6}{\partial S_h} & \frac{\partial\Theta_6}{\partial V_h} & \frac{\partial\Theta_6}{\partial E_h} & \frac{\partial\Theta_6}{\partial I_h} & \frac{\partial\Theta_6}{\partial H_h} & \frac{\partial\Theta_6}{\partial R_h} & \frac{\partial\Theta_6}{\partial S_v} & \frac{\partial\Theta_6}{\partial E_v} & \frac{\partial\Theta_6}{\partial I_v}\\
\frac{\partial\Theta_7}{\partial S_h} & \frac{\partial\Theta_7}{\partial V_h} & \frac{\partial\Theta_7}{\partial E_h} & \frac{\partial\Theta_7}{\partial I_h} & \frac{\partial\Theta_7}{\partial H_h} & \frac{\partial\Theta_7}{\partial R_h} & \frac{\partial\Theta_7}{\partial S_v} & \frac{\partial\Theta_7}{\partial E_v} & \frac{\partial\Theta_7}{\partial I_v}\\
\frac{\partial\Theta_8}{\partial S_h} & \frac{\partial\Theta_8}{\partial V_h} & \frac{\partial\Theta_8}{\partial E_h} & \frac{\partial\Theta_8}{\partial I_h} & \frac{\partial\Theta_8}{\partial H_h} & \frac{\partial\Theta_8}{\partial R_h} & \frac{\partial\Theta_8}{\partial S_v} & \frac{\partial\Theta_8}{\partial E_v} & \frac{\partial\Theta_8}{\partial I_v}\\
\frac{\partial\Theta_9}{\partial S_h} & \frac{\partial\Theta_9}{\partial V_h} & \frac{\partial\Theta_9}{\partial E_h} & \frac{\partial\Theta_9}{\partial I_h} & \frac{\partial\Theta_9}{\partial H_h} & \frac{\partial\Theta_9}{\partial R_h} & \frac{\partial\Theta_9}{\partial S_v} & \frac{\partial\Theta_9}{\partial E_v} & \frac{\partial\Theta_9}{\partial I_v}
\end{pmatrix}.$$

Computing the partial derivatives yields

$$J(E) = \begin{pmatrix}
-(abI_v^0 + d_h + \nu) & 0 & 0 & 0 & 0 & 0 & 0 & 0 & -abS_h^0\\
\nu & -d_h & 0 & 0 & 0 & 0 & 0 & 0 & 0\\
abI_v^0 & 0 & -(\eta_1 + \sigma + d_h) & 0 & 0 & 0 & 0 & 0 & 0\\
0 & 0 & \eta_1 & -(\theta + \delta + d_h) & 0 & 0 & 0 & 0 & 0\\
0 & 0 & 0 & \delta & -(\gamma + d_h) & 0 & 0 & 0 & 0\\
0 & 0 & \sigma & \theta & \gamma & -d_h & 0 & 0 & 0\\
0 & 0 & 0 & -acS_v^0 & 0 & 0 & -(acI_h^0 + d_v) & 0 & 0\\
0 & 0 & 0 & acS_v^0 & 0 & 0 & acI_h^0 & -(d_v + \eta_2) & 0\\
0 & 0 & 0 & 0 & 0 & 0 & 0 & \eta_2 & -(\xi + d_v)
\end{pmatrix}.$$

Evaluating the Jacobian matrix at the disease-free equilibrium E_0, where $S_h^0 = \frac{\tau_h}{d_h+\nu}$and $S_v^0 = \frac{\tau_v}{d_v}$, we obtain

$$J(E^0) = \begin{pmatrix} -(d_h+\nu) & 0 & 0 & 0 & 0 & 0 & 0 & 0 & -\frac{ab\tau_h}{d_h+\nu} \\ \nu & -d_h & 0 & 0 & 0 & 0 & 0 & 0 & 0 \\ 0 & 0 & -(\eta_1+\sigma+d_h) & 0 & 0 & 0 & 0 & 0 & 0 \\ 0 & 0 & \eta_1 & -(\theta+\delta+d_h) & 0 & 0 & 0 & 0 & 0 \\ 0 & 0 & 0 & \delta & -(\gamma+d_h) & 0 & 0 & 0 & 0 \\ 0 & 0 & \sigma & \theta & \gamma & -d_h & 0 & 0 & 0 \\ 0 & 0 & 0 & -\frac{ac\tau_v}{d_v} & 0 & 0 & -d_v & 0 & 0 \\ 0 & 0 & 0 & \frac{ac\tau_v}{d_v} & 0 & 0 & 0 & -(d_v+\eta_2) & 0 \\ 0 & 0 & 0 & 0 & 0 & 0 & 0 & \eta_2 & -(\xi+d_v) \end{pmatrix}.$$

For the local stability of the disease-free equilibrium E^0, it is necessary that the trace and determinant of the Jacobian matrix evaluated at E^0 satisfy

$$\mathrm{Tr}\,(J_{E^0}) < 0 \quad \text{and} \quad \det(J_{E^0}) > 0.$$

The trace of the Jacobian matrix at E^0 is given by

$$\begin{aligned} \mathrm{Tr}\,(J_{E^0}) &= -(d_h+\nu) - d_h - (\eta_1+\sigma+d_h) - (\theta+\delta+d_h) - (\gamma+d_h) - d_h - d_v - (d_v+\eta_2) - (\xi+d_v), \\ &= -\theta - \sigma - \gamma - \delta - \nu - \xi - \eta_1 - \eta_2 - 6d_h - 3d_v < 0. \end{aligned} \tag{6.1}$$

The determinant of the Jacobian matrix at E^0 is computed using *Mathematica* and is given by

$$\det(J_{E^0}) = d_h^2(d_h+\nu)(\eta_1+\sigma+d_h)(\theta+\delta+d_h)(\gamma+d_h)(d_v+\eta_2)(\xi+d_v) > 0.$$

Since $\mathrm{Tr}\,(J_{E^0}) < 0$ and $\det(J_{E^0}) > 0$, it follows that the disease-free equilibrium E^0 is LAS when $\mathcal{R}_0 < 1$, and becomes unstable otherwise

Theorem 6.2. *If $\mathcal{R}_0 > 1$, then the EE point $E^\star$ is GAS.*

Proof. We define the nonlinear Lyapunov function as:

$$L(t) = \mathscr{N}_h(t) + \mathscr{N}_v(t), \tag{6.2}$$

where

$$\begin{aligned} N_h &= N_1(S_h - S_h^\star - S_h^\star In\frac{S_h}{S_h^\star}) + N_2(V_h - V_h^\star - V_h^\star In\frac{V_h}{V_h^\star}) + N_3(E_h - E_h^\star - E_h^\star In\frac{E_h}{E_h^\star}) \\ &\quad + N_4(I_h - I_h^\star - I_h^\star In\frac{I_h}{I_h^\star}) + N_5(H_h - H_h^\star - H_h^\star In\frac{H_h}{H_h^\star}), \\ N_v &= N_7(S_v - S_v^\star - S_v^\star In\frac{S_v}{S_v^\star}) + N_8(E_v - E_v^\star - E_v^\star In\frac{E_v}{E_v^\star}) + N_9(I_v - I_v^\star - I_v^\star In\frac{I_v}{I_v^\star}). \end{aligned}$$

The Caputo fractional derivative corresponding to Eq (6.2) is expressed as

$${}^{\mathscr{C}}\mathscr{D}_t^\zeta L(t) = {}^{\mathscr{C}}\mathscr{D}_t^\zeta N_h(t) + {}^{\mathscr{C}}\mathscr{D}_t^\zeta N_v(t). \tag{6.3}$$

It follows that

$$
\begin{aligned}
{}^{\mathscr{C}}\mathscr{D}^{\zeta}L(t) &= N_1(1-\frac{S_h^\star}{S_h})^{C}D_t^{\zeta}S_h + N_2(1-\frac{V_h^\star}{V_h})^{\mathscr{C}}\mathscr{D}_t^{\zeta}V_h + N_3(1-\frac{E_h^\star}{E_h})^{\mathscr{C}}\mathscr{D}_t^{\zeta}E_h + N_4(1-\frac{I_h^\star}{I_h})^{\mathscr{C}}\mathscr{D}_t^{\zeta}I_h \\
&+ N_5(1-\frac{H_h^\star}{H_h})^{\mathscr{C}}\mathscr{D}_t^{\zeta}H_h + N_6(1-\frac{R_h^\star}{R_h})^{\mathscr{C}}\mathscr{D}_t^{\zeta}R_h + N_7(1-\frac{S_v^\star}{S_v})^{\mathscr{C}}\mathscr{D}_t^{\zeta}S_v + N_8(1-\frac{E_v^\star}{E_v})^{\mathscr{C}}\mathscr{D}_t^{\zeta}E_v \\
&+ N_9(1-\frac{I_v^\star}{I_v})^{\mathscr{C}}\mathscr{D}_t^{\zeta}I_v. \qquad (6.4)
\end{aligned}
$$

Using system (3.2) in Eq (6.4), the resulting expression is

$$
\begin{aligned}
{}^{\mathscr{C}}\mathscr{D}^{\zeta}L(t) &= N_1(1-\frac{S_h^\star}{S_h})(\tau_h-(abI_v+d_h+\nu)S_h) + N_2(1-\frac{V_h^\star}{V_h})^{\mathscr{C}}\mathscr{D}_t^{\zeta}(\nu S_h - d_hV_h) \\
&+ N_3(1-\frac{E_h^\star}{E_h})(abI_vS_h-(\eta_1+\sigma+d_h)E_h) + N_4(1-\frac{I_h^\star}{I_h})(\eta_1E_h-(\theta+\delta+d_h)I_h) \\
&+ N_5(1-\frac{H_h^\star}{H_h})(\delta I_h-(\gamma+d_h)H_h) + N_6(1-\frac{R_h^\star}{R_h})(\sigma E_h+\theta I_h+\gamma H_h-d_hR_h) \\
&+ N_7(1-\frac{S_v^\star}{S_v})(\tau_v-(acI_h+d_v)S_v) + N_8(1-\frac{E_v^\star}{E_v})(acI_hS_v-(d_v+\eta_2)E_v) \\
&+ N_9(1-\frac{I_v^\star}{I_v})(\eta_2E_v-(\xi+d_v)I_v). \qquad (6.5)
\end{aligned}
$$

Rewriting Eq (6.5) by reorganizing its terms

$$
\begin{aligned}
{}^{\mathscr{C}}\mathscr{D}^{\zeta}L(t) &= (\nu+d_h)\,S_h^\star(3-\frac{V_h}{V_h^\star}-\frac{V_h^\star S_h}{V_hS_h^\star}-\frac{S_h^\star}{S_h}) + \frac{d_vbI_v^\star S_h^\star}{cI_h^\star}(2-\frac{S_v}{S_v^\star}-\frac{S_v^\star}{S_v}) \\
&+ abI_v^\star S_h^\star(3-\frac{S_vE_v^\star}{S_v^\star E_v}-\frac{E_v}{E_v^\star}-\frac{S_v^\star}{S_v}). \qquad (6.6)
\end{aligned}
$$

Through the use of the arithmetic–geometric mean inequality, the inequalities in Eq (6.6) are established as follows:

$$
\begin{aligned}
&3-\frac{V_h}{V_h^\star}-\frac{V_h^\star S_h}{V_hS_h^\star}-\frac{S_h^\star}{S_h}\le 0,\\
&2-\frac{S_v}{S_v^\star}-\frac{S_v^\star}{S_v}\le 0,\\
&3-\frac{S_vE_v^\star}{S_v^\star E_v}-\frac{E_v}{E_v^\star}-\frac{S_v^\star}{S_v}.
\end{aligned}
$$

Hence, ${}^{\mathscr{C}}D_t^{\zeta}L \le 0$ for $\mathcal{R}_0 > 1$, with equality holding only at $S_h = S_h^\star$, $V_h = V_h^\star$, $S_v = S_v^\star$, and $E_v = E_v^\star$. By LaSalle's invariance principle, it follows that for $R_0 > 1$, the solution trajectories originating from any initial condition in Ω converge to the persistent-infection equilibrium. This establishes the global asymptotic stability of the endemic state.

7. Sensitivity analysis

The sensitivity indices $\Theta_p^{\mathcal{R}_0}$ indicate the relative change in the $\mathcal{R}_0$ with respect to changes in model parameters p. The computed indices are as follows:

$$\Theta_p^{\mathcal{R}_0} = \frac{\partial \mathcal{R}_0}{p} \times \frac{p}{\mathcal{R}_0} \tag{7.1}$$

Using Eq (7.1), we calculate the sensitivity indices, which are presented in Table 1. From the results, the biting rate a has the highest positive sensitivity index (+1), indicating that it is the most influential parameter in causing the spread of the disease. This indicates that increased contact between vectors and humans increases transmission. Similarly, the human recruitment rate τ_h, vector recruitment rate τ_v, and transmission probabilities b and c all have positive indices (+0.5), showing that these parameters contribute to increasing disease prevalence.

In contrast, the vaccination rate ν has a strong negative sensitivity index (−0.49), highlighting its important role in disease control by reducing $\mathcal{R}_0$. Other parameters associated with recovery or removal, including the exposed recovery rate σ, hospitalization rate δ, infectious recovery rate θ, vector death rate d_v, and disease-induced vector death rate ξ, also exhibit negative sensitivity indices. This suggests that enhancing the recovery or mortality of infected individuals and vectors effectively slows the transmission of TBE disease.

8. Numerical method

In this section, we construct a numerical scheme based on the Caputo fractional derivative to discretize the system of FDEs, with the Adams-Bashforth method extended to account for memory effects. This approach (see Ref [44]) effectively captures the hereditary and nonlocal dynamics inherent in the fractional-order model:

$${}^{\mathscr{C}}\mathscr{D}_t^{\zeta} = g(t, \jmath(t)) = \frac{1}{\Gamma(\zeta)} \int_0^t g(\ell, \jmath(\ell))(t-\ell)^{\zeta-1} d\ell. \tag{8.1}$$

Proceeding with the fundamental theorem of calculus on Eq (8.1), we derive

$$\jmath(t) - \jmath(0) = \frac{1}{\Gamma(\zeta)} \int_0^t g(\ell, \jmath(\ell))(t-\ell)^{\zeta-1} d\tau, \tag{8.2}$$

therefore, for $t = t_{m+1}$

$$\jmath(t_{m+1}) - \jmath(0) = \frac{1}{\Gamma(\zeta)} \int_0^{t_{m+1}} (t_{m+1}-t)^{\zeta-1} g(t, \jmath(t)) dt, \tag{8.3}$$

and

$$\jmath(t_m) - \jmath(0) = \frac{1}{\Gamma(\zeta)} \int_0^{t_m} (t_m-t)^{\zeta-1} g(t, \jmath(t)) dt. \tag{8.4}$$

Computing the difference between Eqs (8.3) and (8.4) leads to

$$\jmath(t_{m+1}) = \jmath(t_m) + \frac{1}{\Gamma(\zeta)} \int_0^{t_{m+1}} (t_{m+1}-t)^{\zeta-1} g(t, \jmath(t)) + \frac{1}{\Gamma(\zeta)} \int_0^{t_m} (t_m-t)^{\zeta-1} g(t, \jmath(t)) dt. \tag{8.5}$$

It follows that Eq (8.5) becomes

$$\jmath(t_{m+1}) = \jmath(t_m) + \mathscr{A}_{\zeta,1} + \mathscr{A}_{\zeta,2}t, \tag{8.6}$$

where

$$\mathscr{A}_{\zeta,1} = \frac{1}{\Gamma(\zeta)} \int_0^{t_{m+1}} (t_{m+1} - t)^{\zeta-1} g(t, \jmath(t))dt \tag{8.7}$$

and

$$\mathscr{A}_{\zeta,2} = \frac{1}{\Gamma(\zeta)} \int_0^{t_m} (t_m - t)^{\zeta-1} g(t, \jmath(t))dt. \tag{8.8}$$

The Lagrange interpolating polynomial for $g(t, \jmath(t))$ is

$$\begin{aligned} p(t) &\simeq \frac{t - t_{m-1}}{t_m - t_{m-1}} g(t_m, \jmath_m) + \frac{t - t_m}{t_{m-1} - t_m} g(t_{m-1}, \jmath_{m-1}), \\ p(t) &= \frac{g(t_m, \jmath_m)}{h}(t - t_{m-1}) - \frac{g(t_{m-1}, \jmath_{m-1})}{h}(t - t_m). \end{aligned} \tag{8.9}$$

This leads to

$$\begin{aligned} \mathscr{A}_{\zeta,1} &= \frac{g(t_m, \jmath_m)}{h\Gamma(\zeta)} \int_0^{t_{m+1}} (t_{m+1} - t)^{\zeta-1}(t - t_{m-1})dt - \frac{g(t_{m-1}, \jmath_{m-1})}{h\Gamma(\zeta)} \int_0^{t_{m+1}} (t_{m+1} - t)(t - t_m)dt, \\ \mathscr{A}_{\zeta,1} &= \frac{g(t_m, \jmath_m)}{h\Gamma(\zeta)} \int_0^{t_{m+1}} \jmath^{\zeta-1}(t_{m+1} - \jmath - t_{m-1})dy - \frac{g(t_{m-1}, \jmath_{m-1})}{h\Gamma(\zeta)} \int_0^{t_{m+1}} \jmath^{\zeta-1}(t_{m+1} - \jmath - t_m)dy. \end{aligned} \tag{8.10}$$

Hence,

$$\mathscr{A}_{\zeta,1} = \frac{g(t_m, \jmath_m)}{h\Gamma(\zeta)} \left\{ \frac{2ht_{m+1}^{\zeta}}{\zeta} - \frac{t_{m+1}^{\zeta+1}}{\zeta+1} \right\} - \frac{g(t_{m-1}, \jmath_{m-1})}{h\Gamma(\zeta)} \left\{ \frac{ht_{m+1}^{\zeta}}{\zeta} - \frac{t_{m+1}^{\zeta+1}}{\zeta+1} \right\}. \tag{8.11}$$

Proceeding in a similar manner, we find

$$\begin{aligned} \mathscr{A}_{\zeta,2} &= \frac{g(t_m, \jmath_m)}{h\Gamma(\zeta)} \int_0^{t_m} (t_m - t)^{\zeta-1}(t - t_{m-1})dt - \frac{(t_{m-1}, \jmath_{m-1})}{h\Gamma(\zeta)} \int_0^{t_m} (t_m - t)^{\zeta-1}(t - t_m)dt, \\ \mathscr{A}_{\zeta,2} &= \frac{g(t_m, \jmath_m)}{h\Gamma(\zeta)} \int_0^{t_m} \jmath^{\zeta-1}(t_m - \jmath - t_{m-1})dy - \frac{g(t_{m-1}, \jmath_{m-1})}{h\Gamma(\zeta)} \frac{t_m^{\zeta+1}}{\zeta}, \\ \mathscr{A}_{\zeta,2} &= \frac{g(t_m, \jmath_m)}{h\Gamma(\zeta)} \left\{ \frac{ht_m^{\zeta}}{\zeta} - \frac{t_m^{\zeta+1}}{\zeta+1} \right\} + \frac{g(t_{m-1}, \jmath_{m-1})}{h\Gamma(\zeta+1)} t_{\zeta}^{\zeta+1}. \end{aligned} \tag{8.12}$$

Applying Eqs (8.11) and (8.12) to Eq (8.6), the approximation becomes

$$\begin{aligned} \jmath(t_{m+1}) = \jmath(t_m) &+ \frac{g(t_m, \jmath_m)}{h\Gamma(\zeta)} \left\{ \frac{2ht_{m+1}^{\zeta}}{\zeta} - \frac{t_{m+1}^{\zeta+1}}{\zeta+1} + \frac{ht_m^{\zeta}}{\zeta} - \frac{t_m^{\zeta+1}}{\zeta+1} \right\} \\ &+ \frac{g(t_{m-1}, \jmath_{m-1})}{h\Gamma(\zeta)} \left\{ \frac{ht_{m+1}^{\zeta}}{\zeta} - \frac{t_{m+1}^{\zeta+1}}{\zeta+1} + \frac{t_m^{\zeta}}{\zeta+1} \right\}. \end{aligned} \tag{8.13}$$

Theorem 8.1. *The numerical approximation of $\jmath(t)$ for the Caputo fractional differential equation ${}^{\mathscr{C}}\mathscr{D}_t^{\zeta} = g(t, \jmath(t))$, with bounded g, is represented by*

$$\jmath(t_{m+1}) = \jmath(t_m) + \frac{g(t_m, \jmath_m)}{h\Gamma(\zeta)}\left\{\frac{2ht_{m+1}^{\zeta}}{\zeta} - \frac{t_{m+1}^{\zeta+1}}{\zeta+1} + \frac{ht_m^{\zeta}}{\zeta} - \frac{t_m^{\zeta+1}}{\zeta+1}\right\}$$
$$+ \frac{g(t_{m-1}, \jmath_{m-1})}{h\Gamma(\zeta)}\left\{\frac{ht_{m+1}^{\zeta}}{\zeta} - \frac{t_{m+1}^{\zeta+1}}{\zeta+1} + \frac{t_m^{\zeta}}{\zeta+1}\right\} + R_m^{\zeta}(t),$$

where

$$R_m^{\zeta}(t) < \frac{h^{3+\zeta}M}{12\Gamma(\zeta+1)}\{(n+1)^{\zeta} + n^2\}.$$

The fundamental theorem of analysis is employed for system (3.2) to derive governing equations for the G_i kernels. These kernels correspond to $\mathscr{K}_i = 1, \ldots, 9$. Consequently, we obtain

$$\begin{aligned}
S_h(t) - S_h(0) &= \frac{1}{\Gamma(\zeta)}\int_0^t \mathscr{K}_1(\ell, S_h(t))(t-\ell)^{\zeta-1}d\tau,\\
V_h(t) - V_h(0) &= \frac{1}{\Gamma(\zeta)}\int_0^t \mathscr{K}_2(\ell, V_h(t))(t-\ell)^{\zeta-1}d\tau,\\
E_h(t) - E_h(0) &= \frac{1}{\Gamma(\zeta)}\int_0^t \mathscr{K}_3(\ell, E_h(t))(t-\ell)^{\zeta-1}d\tau,\\
I_h(t) - I_h(0) &= \frac{1}{\Gamma(\zeta)}\int_0^t \mathscr{K}_4(\ell, I_h(t))(t-\ell)^{\zeta-1}d\tau,\\
H_h(t) - V(0) &= \frac{1}{\Gamma(\zeta)}\int_0^t \mathscr{K}_5(\ell, H_h(t))(t-\ell)^{\zeta-1}d\tau,\\
R_h(t) - R_h(0) &= \frac{1}{\Gamma(\zeta)}\int_0^t \mathscr{K}_6(\ell, R_h(t))(t-\ell)^{\zeta-1}d\tau,\\
S_v(t) - S_v(0) &= \frac{1}{\Gamma(\zeta)}\int_0^t \mathscr{K}_7(\ell, S_v(t))(t-\ell)^{\zeta-1}d\tau,\\
E_v(t) - E_v(0) &= \frac{1}{\Gamma(\zeta)}\int_0^t \mathscr{K}_8(\ell, E_v(t))(t-\ell)^{\zeta-1}d\tau,\\
I_v(t) - I_v(0) &= \frac{1}{\Gamma(\zeta)}\int_0^t \mathscr{K}_9(\ell, I_v(t))(t-\ell)^{\zeta-1}d\tau,
\end{aligned} \tag{8.14}$$

Consequently, the following holds at $t = t_{m+1}$:

$$\begin{aligned}
S_h(t_m) - S_h(0) &= \frac{1}{\Gamma(\zeta)}\int_0^{t_{m+1}} (t_{m+1}-t)^{\zeta-1} g(t, S_h(t))dt,\\
V_h(t_{m+1}) - V_h(0) &= \frac{1}{\Gamma(\zeta)}\int_0^{t_{m+1}} (t_{m+1}-t)^{\zeta-1} g(t, V_h(t))dt,\\
E_h(t_{m+1}) - E_h(0) &= \frac{1}{\Gamma(\zeta)}\int_0^{t_{m+1}} (t_{m+1}-t)^{\zeta-1} g(t, E_h(t))dt,\\
I_h(t_{m+1}) - I_h(0) &= \frac{1}{\Gamma(\zeta)}\int_0^{t_{m+1}} (t_{m+1}-t)^{\zeta-1} g(t, I_h(t))dt,
\end{aligned}$$

$$
\begin{aligned}
H_h(t_{m+1}) - H_h(0) &= \frac{1}{\Gamma(\zeta)} \int_0^{t_{m+1}} (t_{m+1} - t)^{\zeta-1} g(t, H_h(t))dt,\\
R_h(t_{m+1}) - R_h(0) &= \frac{1}{\Gamma(\zeta)} \int_0^{t_{m+1}} (t_{m+1} - t)^{\zeta-1} g(t, R_h(t))dt,\\
S_v(t_{m+1}) - S_v(0) &= \frac{1}{\Gamma(\zeta)} \int_0^{t_{m+1}} (t_{m+1} - t)^{\zeta-1} g(t, S_v(t))dt,\\
E_v(t_{m+1}) - E_v(0) &= \frac{1}{\Gamma(\zeta)} \int_0^{t_{m+1}} (t_{m+1} - t)^{\zeta-1} g(t, E_v(t))dt,\\
I_v(t_{m+1}) - I_v(0) &= \frac{1}{\Gamma(\zeta)} \int_0^{t_{m+1}} (t_{m+1} - t)^{\zeta-1} g(t, I_v(t))dt.
\end{aligned} \tag{8.15}
$$

and

$$
\begin{aligned}
S_h(t_m) - S_h(0) &= \frac{1}{\Gamma(\zeta)} \int_0^{t_m} (t_m - t)^{\zeta-1} g(t, S_h(t))dt,\\
V_h(t_m) - V_h(0) &= \frac{1}{\Gamma(\zeta)} \int_0^{t_m} (t_m - t)^{\zeta-1} g(t, V_h(t))dt,\\
E_h(t_m) - E_h(0) &= \frac{1}{\Gamma(\zeta)} \int_0^{t_m} (t_m - t)^{\zeta-1} g(t, E_h(t))dt,\\
I_h(t_m) - I_h(0) &= \frac{1}{\Gamma(\zeta)} \int_0^{t_m} (t_m - t)^{\zeta-1} g(t, I_h(t))dt,\\
H_h(t_m) - H_h(0) &= \frac{1}{\Gamma(\zeta)} \int_0^{t_m} (t_m - t)^{\zeta-1} g(t, H_h(t))dt,\\
R_h(t_m) - R_h(0) &= \frac{1}{\Gamma(\zeta)} \int_0^{t_m} (t_m - t)^{\zeta-1} g(t, R_h(t))dt,\\
S_v(t_m) - S_v(0) &= \frac{1}{\Gamma(\zeta)} \int_0^{t_m} (t_m - t)^{\zeta-1} g(t, S_v(t))dt,\\
E_v(t_m) - E_v(0) &= \frac{1}{\Gamma(\zeta)} \int_0^{t_m} (t_m - t)^{\zeta-1} g(t, E_v(t))dt,\\
I_v(t_m) - I_v(0) &= \frac{1}{\Gamma(\zeta)} \int_0^{t_m} (t_m - t)^{\zeta-1} g(t, I_v(t))dt.
\end{aligned} \tag{8.16}
$$

Subtracting Eq (8.16) from Eq (8.15) yields

$$
\begin{aligned}
S_h(t_{m+1}) - S_h(t_m) &= \frac{1}{\Gamma(\zeta)} \int_0^{t_{m+1}} (t_{m+1} - t)^{\zeta-1} \mathscr{K}_1(t, S_h(t)) + \frac{1}{\Gamma(\zeta)} \int_0^{t_m} (t_m - t)^{\zeta-1} \mathscr{K}_1(t, S_h(t))dt,\\
V_h(t_{m+1}) - V_h(t_m) &= \frac{1}{\Gamma(\zeta)} \int_0^{t_{m+1}} (t_{m+1} - t)^{\zeta-1} \mathscr{K}_2(t, V_h(t)) + \frac{1}{\Gamma(\zeta)} \int_0^{t_m} (t_m - t)^{\zeta-1} \mathscr{K}_2(t, V_h(t))dt,\\
E_h(t_{m+1}) - E_h(t_m) &= \frac{1}{\Gamma(\zeta)} \int_0^{t_{m+1}} (t_{m+1} - t)^{\zeta-1} \mathscr{K}_3(t, E_h(t)) + \frac{1}{\Gamma(\zeta)} \int_0^{t_m} (t_m - t)^{\zeta-1} \mathscr{K}_3(t, E_h(t))dt,\\
I_h(t_{m+1}) - V(t_m) &= \frac{1}{\Gamma(\zeta)} \int_0^{t_{m+1}} (t_{m+1} - t)^{\zeta-1} \mathscr{K}_4(t, I_h(t)) + \frac{1}{\Gamma(\zeta)} \int_0^{t_m} (t_m - t)^{\zeta-1} \mathscr{K}_4(t, I_h(t))dt,\\
H_h(t_{m+1}) - H_h(t_m) &= \frac{1}{\Gamma(\zeta)} \int_0^{t_{m+1}} (t_{m+1} - t)^{\zeta-1} \mathscr{K}_5(t, H_h(t)) + \frac{1}{\Gamma(\zeta)} \int_0^{t_m} (t_m - t)^{\zeta-1} \mathscr{K}_5(t, H_h(t))dt,
\end{aligned}
$$

$$
\begin{aligned}
R_h(t_{m+1}) - R_h(t_m) &= \frac{1}{\Gamma(\zeta)}\int_0^{t_{m+1}} (t_{m+1}-t)^{\zeta-1}\mathscr{K}_6(t,R_h(t)) + \frac{1}{\Gamma(\zeta)}\int_0^{t_m} (t_m-t)^{\zeta-1}\mathscr{K}_6(t,R_h(t))dt,\\
S_v(t_{m+1}) - S_v(t_m) &= \frac{1}{\Gamma(\zeta)}\int_0^{t_{m+1}} (t_{m+1}-t)^{\zeta-1}\mathscr{K}_7(t,S_v(t)) + \frac{1}{\Gamma(\zeta)}\int_0^{t_m} (t_m-t)^{\zeta-1}\mathscr{K}_7(t,S_v(t))dt,\\
E_h(t_{m+1}) - E_h(t_m) &= \frac{1}{\Gamma(\zeta)}\int_0^{t_{m+1}} (t_{m+1}-t)^{\zeta-1}\mathscr{K}_8(t,E_h(t)) + \frac{1}{\Gamma(\zeta)}\int_0^{t_m} (t_m-t)^{\zeta-1}\mathscr{K}_8(t,E_h(t))dt,\\
I_v(t_{m+1}) - I_v(t_m) &= \frac{1}{\Gamma(\zeta)}\int_0^{t_{m+1}} (t_{m+1}-t)^{\zeta-1}\mathscr{K}_9(t,I_v(t)) + \frac{1}{\Gamma(\zeta)}\int_0^{t_m} (t_m-t)^{\zeta-1}\mathscr{K}_9(t,I_v(t))dt. \qquad (8.17)
\end{aligned}
$$

Upon expressing Eq (8.17) in the form of Eq (8.13), the following result is obtained

$$
\begin{aligned}
S_h(t_{m+1}) &= S_h(t_m) + \frac{g(t_m,S_{h,m})}{h\Gamma(\zeta)}\left\{\frac{2ht_{m+1}^{\zeta}}{\zeta} - \frac{t_{m+1}^{\zeta+1}}{\zeta+1} + \frac{ht_m^{\zeta}}{\zeta} - \frac{t_m^{\zeta+1}}{\zeta+1}\right\} + \frac{g(t_{m-1},S_{h,m-1})}{h\Gamma(\zeta)}\left\{\frac{ht_{m+1}^{\zeta}}{\zeta} - \frac{t_{m+1}^{\zeta+1}}{\zeta+1} + \frac{t_m^{\zeta}}{\zeta+1}\right\},\\
V_h(t_{m+1}) &= V_h(t_m) + \frac{g(t_m,V_{h,m})}{h\Gamma(\zeta)}\left\{\frac{2ht_{m+1}^{\zeta}}{\zeta} - \frac{t_{m+1}^{\zeta+1}}{\zeta+1} + \frac{ht_m^{\zeta}}{\zeta} - \frac{t_m^{\zeta+1}}{\zeta+1}\right\} + \frac{g(t_{m-1},V_{h,m-1})}{h\Gamma(\zeta)}\left\{\frac{ht_{m+1}^{\zeta}}{\zeta} - \frac{t_{m+1}^{\zeta+1}}{\zeta+1} + \frac{t_m^{\zeta}}{\zeta+1}\right\},\\
E_h(t_{m+1}) &= E_h(t_m) + \frac{g(t_m,E_{h,m})}{h\Gamma(\zeta)}\left\{\frac{2ht_{m+1}^{\zeta}}{\zeta} - \frac{t_{m+1}^{\zeta+1}}{\zeta+1} + \frac{ht_m^{\zeta}}{\zeta} - \frac{t_m^{\zeta+1}}{\zeta+1}\right\} + \frac{g(t_{m-1},E_{h,m-1})}{h\Gamma(\zeta)}\left\{\frac{ht_{m+1}^{\zeta}}{\zeta} - \frac{t_{m+1}^{\zeta+1}}{\zeta+1} + \frac{t_m^{\zeta}}{\zeta+1}\right\},\\
I_h(t_{m+1}) &= I_h(t_m) + \frac{g(t_m,I_{h,m})}{h\Gamma(\zeta)}\left\{\frac{2ht_{m+1}^{\zeta}}{\zeta} - \frac{t_{m+1}^{\zeta+1}}{\zeta+1} + \frac{ht_m^{\zeta}}{\zeta} - \frac{t_m^{\zeta+1}}{\zeta+1}\right\} + \frac{g(t_{m-1},I_{h,m-1})}{h\Gamma(\zeta)}\left\{\frac{ht_{m+1}^{\zeta}}{\zeta} - \frac{t_{m+1}^{\zeta+1}}{\zeta+1} + \frac{t_m^{\zeta}}{\zeta+1}\right\},\\
H_h(t_{m+1}) &= H_h(t_m) + \frac{g(t_m,H_{h,m})}{h\Gamma(\zeta)}\left\{\frac{2ht_{m+1}^{\zeta}}{\zeta} - \frac{t_{m+1}^{\zeta+1}}{\zeta+1} + \frac{ht_m^{\zeta}}{\zeta} - \frac{t_m^{\zeta+1}}{\zeta+1}\right\} + \frac{g(t_{m-1},H_{h,m-1})}{h\Gamma(\zeta)}\left\{\frac{ht_{m+1}^{\zeta}}{\zeta} - \frac{t_{m+1}^{\zeta+1}}{\zeta+1} + \frac{t_m^{\zeta}}{\zeta+1}\right\},\\
R_h(t_{m+1}) &= R_h(t_m) + \frac{g(t_m,R_{h,m})}{h\Gamma(\zeta)}\left\{\frac{2ht_{m+1}^{\zeta}}{\zeta} - \frac{t_{m+1}^{\zeta+1}}{\zeta+1} + \frac{ht_m^{\zeta}}{\zeta} - \frac{t_m^{\zeta+1}}{\zeta+1}\right\} + \frac{g(t_{m-1},R_{h,m-1})}{h\Gamma(\zeta)}\left\{\frac{ht_{m+1}^{\zeta}}{\zeta} - \frac{t_{m+1}^{\zeta+1}}{\zeta+1} + \frac{t_m^{\zeta}}{\zeta+1}\right\},\\
S_v(t_{m+1}) &= S_v(t_m) + \frac{g(t_m,S_{v,m})}{h\Gamma(\zeta)}\left\{\frac{2ht_{m+1}^{\zeta}}{\zeta} - \frac{t_{m+1}^{\zeta+1}}{\zeta+1} + \frac{ht_m^{\zeta}}{\zeta} - \frac{t_m^{\zeta+1}}{\zeta+1}\right\} + \frac{g(t_{m-1},S_{v,m-1})}{h\Gamma(\zeta)}\left\{\frac{ht_{m+1}^{\zeta}}{\zeta} - \frac{t_{m+1}^{\zeta+1}}{\zeta+1} + \frac{t_m^{\zeta}}{\zeta+1}\right\},\\
E_v(t_{m+1}) &= E_v(t_m) + \frac{g(t_m,E_{v,m})}{h\Gamma(\zeta)}\left\{\frac{2ht_{m+1}^{\zeta}}{\zeta} - \frac{t_{m+1}^{\zeta+1}}{\zeta+1} + \frac{ht_m^{\zeta}}{\zeta} - \frac{t_m^{\zeta+1}}{\zeta+1}\right\} + \frac{g(t_{m-1},E_{v,m-1})}{h\Gamma(\zeta)}\left\{\frac{ht_{m+1}^{\zeta}}{\zeta} - \frac{t_{m+1}^{\zeta+1}}{\zeta+1} + \frac{t_m^{\zeta}}{\zeta+1}\right\},\\
I_v(t_{m+1}) &= I_v(t_m) + \frac{g(t_m,I_{v,m})}{h\Gamma(\zeta)}\left\{\frac{2ht_{m+1}^{\zeta}}{\zeta} - \frac{t_{m+1}^{\zeta+1}}{\zeta+1} + \frac{ht_m^{\zeta}}{\zeta} - \frac{t_m^{\zeta+1}}{\zeta+1}\right\} + \frac{g(t_{m-1},I_{v,m-1})}{h\Gamma(\zeta)}\left\{\frac{ht_{m+1}^{\zeta}}{\zeta} - \frac{t_{m+1}^{\zeta+1}}{\zeta+1} + \frac{t_m^{\zeta}}{\zeta+1}\right\}.
\end{aligned} \qquad (8.18)
$$

Using Theorem 8.1, we obtain from Eq (8.18) the following results:

$$
\begin{aligned}
S_h(t_{m+1}) = S_h(t_m) &+ \frac{g(t_m,S_{h,m})}{h\Gamma(\zeta)}\left\{\frac{2ht_{m+1}^{\zeta}}{\zeta} - \frac{t_{m+1}^{\zeta+1}}{\zeta+1} + \frac{ht_m^{\zeta}}{\zeta} - \frac{t_m^{\zeta+1}}{\zeta+1}\right\}\\
&+ \frac{g(t_{m-1},S_{h,m-1})}{h\Gamma(\zeta)}\left\{\frac{ht_{m+1}^{\zeta}}{\zeta} - \frac{t_{m+1}^{\zeta+1}}{\zeta+1} + \frac{t_m^{\zeta}}{\zeta+1}\right\} + {}^1R_m^{\zeta}(t),
\end{aligned}
$$

$$V_h(t_{m+1}) = V_h(t_m) + \frac{g(t_m, V_{h,m})}{h\Gamma(\zeta)}\left\{\frac{2ht_{m+1}^{\zeta}}{\zeta} - \frac{t_{m+1}^{\zeta+1}}{\zeta+1} + \frac{ht_m^{\zeta}}{\zeta} - \frac{t_m^{\zeta+1}}{\zeta+1}\right\}$$
$$+ \frac{g(t_{m-1}, V_{h,m-1})}{h\Gamma(\zeta)}\left\{\frac{ht_{m+1}^{\zeta}}{\zeta} - \frac{t_{m+1}^{\zeta+1}}{\zeta+1} + \frac{t_m^{\zeta}}{\zeta+1}\right\} + {}^2R_m^{\zeta}(t),$$

$$E_h(t_{m+1}) = E_h(t_m) + \frac{g(t_m, E_{h,m})}{h\Gamma(\zeta)}\left\{\frac{2ht_{m+1}^{\zeta}}{\zeta} - \frac{t_{m+1}^{\zeta+1}}{\zeta+1} + \frac{ht_m^{\zeta}}{\zeta} - \frac{t_m^{\zeta+1}}{\zeta+1}\right\}$$
$$+ \frac{g(t_{m-1}, E_{h,m-1})}{h\Gamma(\zeta)}\left\{\frac{ht_{m+1}^{\zeta}}{\zeta} - \frac{t_{m+1}^{\zeta+1}}{\zeta+1} + \frac{t_m^{\zeta}}{\zeta+1}\right\} + {}^3R_m^{\zeta}(t), r$$

$$I_h(t_{m+1}) = I_h(t_m) + \frac{g(t_m, I_{h,m})}{h\Gamma(\zeta)}\left\{\frac{2ht_{m+1}^{\zeta}}{\zeta} - \frac{t_{m+1}^{\zeta+1}}{\zeta+1} + \frac{ht_m^{\zeta}}{\zeta} - \frac{t_m^{\zeta+1}}{\zeta+1}\right\}$$
$$+ \frac{g(t_{m-1}, I_{h,m-1})}{h\Gamma(\zeta)}\left\{\frac{ht_{m+1}^{\zeta}}{\zeta} - \frac{t_{m+1}^{\zeta+1}}{\zeta+1} + \frac{t_m^{\zeta}}{\zeta+1}\right\} + {}^4R_m^{\zeta}(t),$$

$$H_h(t_{m+1}) = H_h(t_m) + \frac{g(t_m, H_{h,m})}{h\Gamma(\zeta)}\left\{\frac{2ht_{m+1}^{\zeta}}{\zeta} - \frac{t_{m+1}^{\zeta+1}}{\zeta+1} + \frac{ht_m^{\zeta}}{\zeta} - \frac{t_m^{\zeta+1}}{\zeta+1}\right\}$$
$$+ \frac{g(t_{m-1}, H_{h,m-1})}{h\Gamma(\zeta)}\left\{\frac{ht_{m+1}^{\zeta}}{\zeta} - \frac{t_{m+1}^{\zeta+1}}{\zeta+1} + \frac{t_m^{\zeta}}{\zeta+1}\right\} + {}^5R_m^{\zeta}(t),$$

$$R_h(t_{m+1}) = R_h(t_m) + \frac{g(t_m, R_{h,m})}{h\Gamma(\zeta)}\left\{\frac{2ht_{m+1}^{\zeta}}{\zeta} - \frac{t_{m+1}^{\zeta+1}}{\zeta+1} + \frac{ht_m^{\zeta}}{\zeta} - \frac{t_m^{\zeta+1}}{\zeta+1}\right\}$$
$$+ \frac{g(t_{m-1}, R_{h,m-1})}{h\Gamma(\zeta)}\left\{\frac{ht_{m+1}^{\zeta}}{\zeta} - \frac{t_{m+1}^{\zeta+1}}{\zeta+1} + \frac{t_m^{\zeta}}{\zeta+1}\right\} + {}^6R_m^{\zeta}(t),$$

$$S_v(t_{m+1}) = S_v(t_m) + \frac{g(t_m, S_{v,m})}{h\Gamma(\zeta)}\left\{\frac{2ht_{m+1}^{\zeta}}{\zeta} - \frac{t_{m+1}^{\zeta+1}}{\zeta+1} + \frac{ht_m^{\zeta}}{\zeta} - \frac{t_m^{\zeta+1}}{\zeta+1}\right\}$$
$$+ \frac{g(t_{m-1}, S_{v,m-1})}{h\Gamma(\zeta)}\left\{\frac{ht_{m+1}^{\zeta}}{\zeta} - \frac{t_{m+1}^{\zeta+1}}{\zeta+1} + \frac{t_m^{\zeta}}{\zeta+1}\right\} + {}^7R_m^{\zeta}(t),$$

$$E_v(t_{m+1}) = E_v(t_m) + \frac{g(t_m, E_{v,m})}{h\Gamma(\zeta)}\left\{\frac{2ht_{m+1}^{\zeta}}{\zeta} - \frac{t_{m+1}^{\zeta+1}}{\zeta+1} + \frac{ht_m^{\zeta}}{\zeta} - \frac{t_m^{\zeta+1}}{\zeta+1}\right\}$$
$$+ \frac{g(t_{m-1}, E_{v,m-1})}{h\Gamma(\zeta)}\left\{\frac{ht_{m+1}^{\zeta}}{\zeta} - \frac{t_{m+1}^{\zeta+1}}{\zeta+1} + \frac{t_m^{\zeta}}{\zeta+1}\right\} + {}^8R_m^{\zeta}(t),$$

$$I_v(t_{m+1}) = I_v(t_m) + \frac{g(t_m, I_{v,m})}{h\Gamma(\zeta)}\left\{\frac{2ht_{m+1}^{\zeta}}{\zeta} - \frac{t_{m+1}^{\zeta+1}}{\zeta+1} + \frac{ht_m^{\zeta}}{\zeta} - \frac{t_m^{\zeta+1}}{\zeta+1}\right\}$$
$$+ \frac{g(t_{m-1}, I_{v,m-1})}{h\Gamma(\zeta)}\left\{\frac{ht_{m+1}^{\zeta}}{\zeta} - \frac{t_{m+1}^{\zeta+1}}{\zeta+1} + \frac{t_m^{\zeta}}{\zeta+1}\right\} + {}^9R_m^{\zeta}(t),$$

where

$$ {}^{i}R_m^{\zeta}(t) < \left(\frac{h^{3+\zeta}M_i}{12\,\Gamma(\zeta+1)}\right)\left\{(n+1)^{\zeta}+n^2\right\}, \quad i=1,2,\ldots,9. $$

9. Numerical results and discussion

In the numerical simulations, model (3.2) is solved using MATLAB over the time interval $t \in [0, 60]$ days. All parameter values used in the simulations are listed in Table 1. As shown in Figure 3, the PRCC values indicate which parameters most strongly influence the basic reproduction number R_0. Positive values increase R_0 and, thus, disease transmission, while negative values indicate parameters that reduce disease spread, highlighting vaccination rate ν and vector death rate d_v as critical control points.

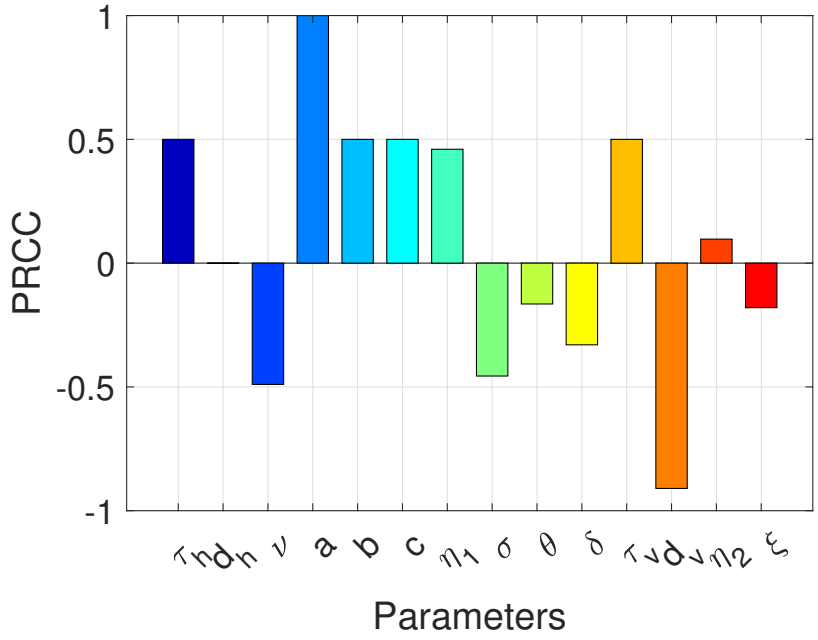

Figure 3. Partial Rank Correlation Coefficient (PRCC) analysis of R_0 with respect to model parameters.

In Figure 4, the 3D plot and contour plot illustrate the combined effects of ν and ξ on $\mathcal{R}_0$, that an increase in ν leads to a marked reduction in $\mathcal{R}_0$, higher values of ξ, correspond to faster loss of immunity, resulting in an increase in $\mathcal{R}_0$. In Figure 5, the interaction between a and ξ, show that an increasing a especially elevates $\mathcal{R}_0$ due to enhanced human-vector contact, and ξ enhances transmission potential by increasing the susceptible population. In Figure 6, a higher recruitment rate leads to an increase in the vector population and a rise in $\mathcal{R}_0$, whereas increasing the death rate d_v reduces transmission. In Figure 7, the effects of b and c, with an increase in either parameter, considerably raising $\mathcal{R}_0$, highlighting the two-way transmission and the need for interventions that reduce transmission efficiency in both directions. Figure 8 show that higher values of η_1 accelerate progression to infectiousness and increase $\mathcal{R}_0$, while increasing σ reduces transmission by removing individuals from the infectious way. Figure 9 illustrates that the faster progression to infectiousness

in vectors enhances transmission and increases $\mathcal{R}_0$, thereby reinforcing the importance of controlling vector transmission efficiency and lifespan.

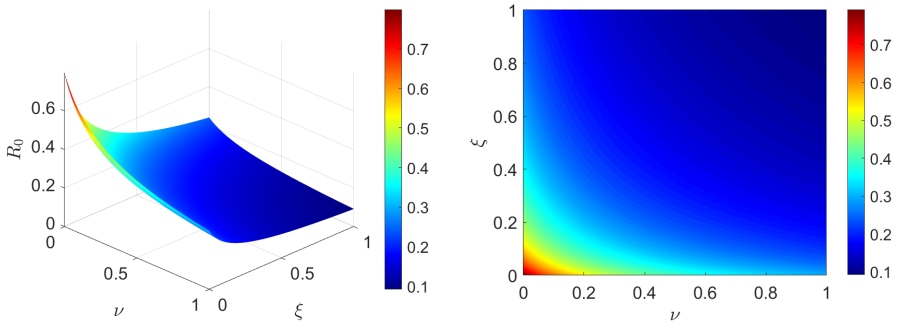

(a) **(b)**

Figure 4. 3D surface and contour plot of $\mathcal{R}_0$ as functions of ν and ξ.

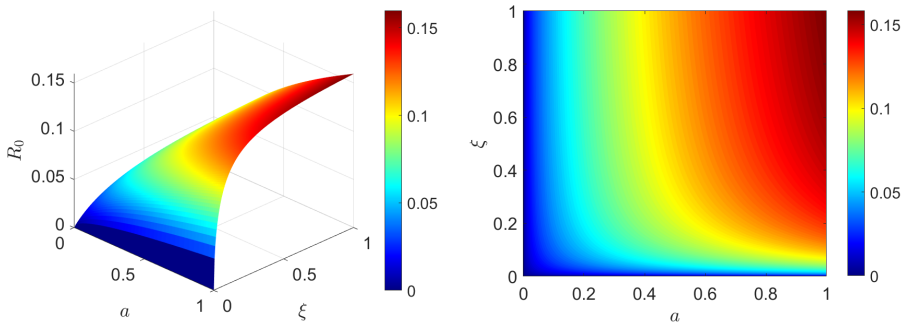

(a) **(b)**

Figure 5. 3D surface and contour plot of $\mathcal{R}_0$ as a and ξ.

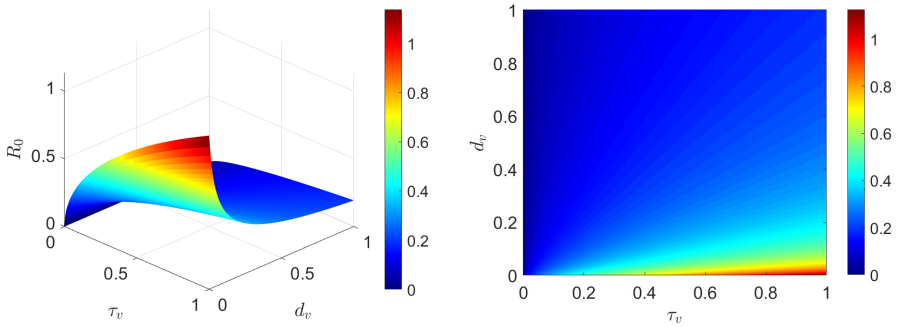

(a) **(b)**

Figure 6. 3D surface and contour plot of $\mathcal{R}_0$ as functions of τ_v and d_v.

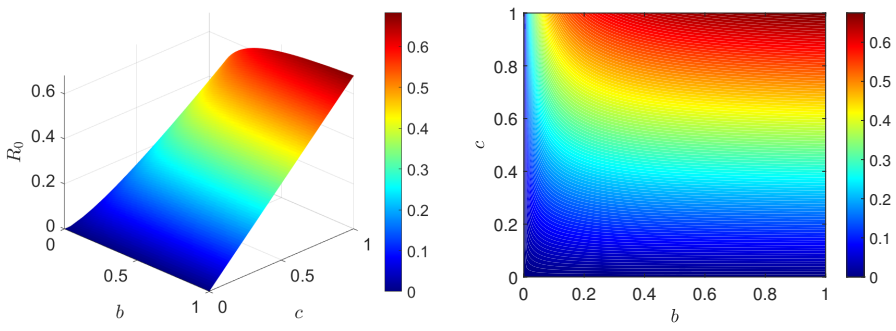

(a) **(b)**

Figure 7. 3D surface and contour plot of $\mathcal{R}_0$ as functions of b and c.

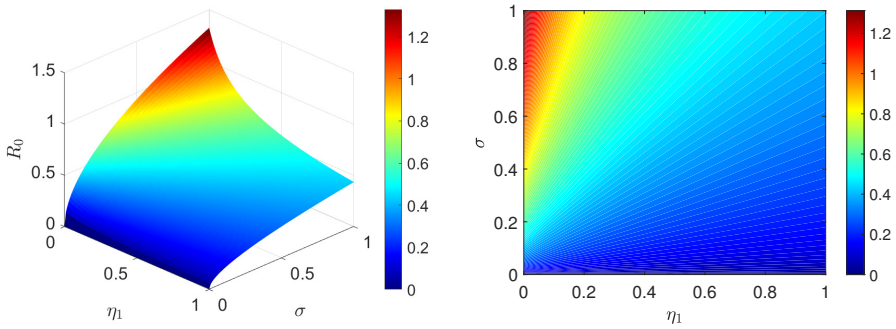

(a) **(b)**

Figure 8. 3D surface and contour plot of $\mathcal{R}_0$ as functions of η_1 and σ.

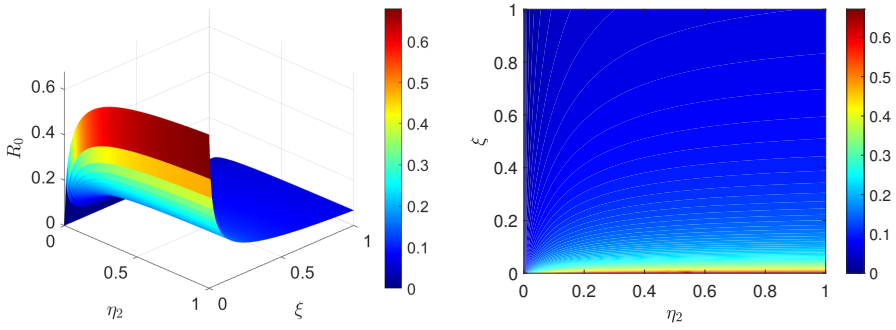

(a) **(b)**

Figure 9. 3D surface and contour plot of $\mathcal{R}_0$ as functions of η_2 and ξ.

Figures 10 and 11 illustrate the temporal evolution of all state variables under different fractional orders ζ and exhibit a slower decay for smaller fractional orders $\zeta \in [0.77, 0.99]$, indicating stronger memory effects in the system. Figure 10(a) shows that the susceptible human population decreases over time, with smaller values of ζ showing a slower decline due to memory effects. Figure 10(b) shows that the vaccinated class increases without decreasing, and its growth is more gradual for lower fractional orders, reflecting delayed vaccination dynamics. Figure 10(c) shows that the exposed human compartment initially increases before becoming stable, while in Figure 10(d), the infectious class shows a short-term rise followed by decay; both dynamics slow down as ζ decreases. Figure 10(e) shows that the hospitalized population H_h follows a delayed peak pattern, with reduced fractional orders extending the persistence of hospitalized individuals. Figure 10(f) shows that the recovered human class increases steadily, with accumulation occurring more slowly for smaller ζ, indicating delayed recovery processes. Figure 11(a) shows that the susceptible vectors decline as infection spreads, with slower dynamics observed for lower fractional orders. Figure 11(b) shows that the exposed vector class increases initially and then levels off, while Figure 11(c) shows that infectious vectors exhibit a gradual rise before stabilization. Therefore, decreasing the fractional order ζ introduces memory effects that slow the progression of human and vector dynamics.

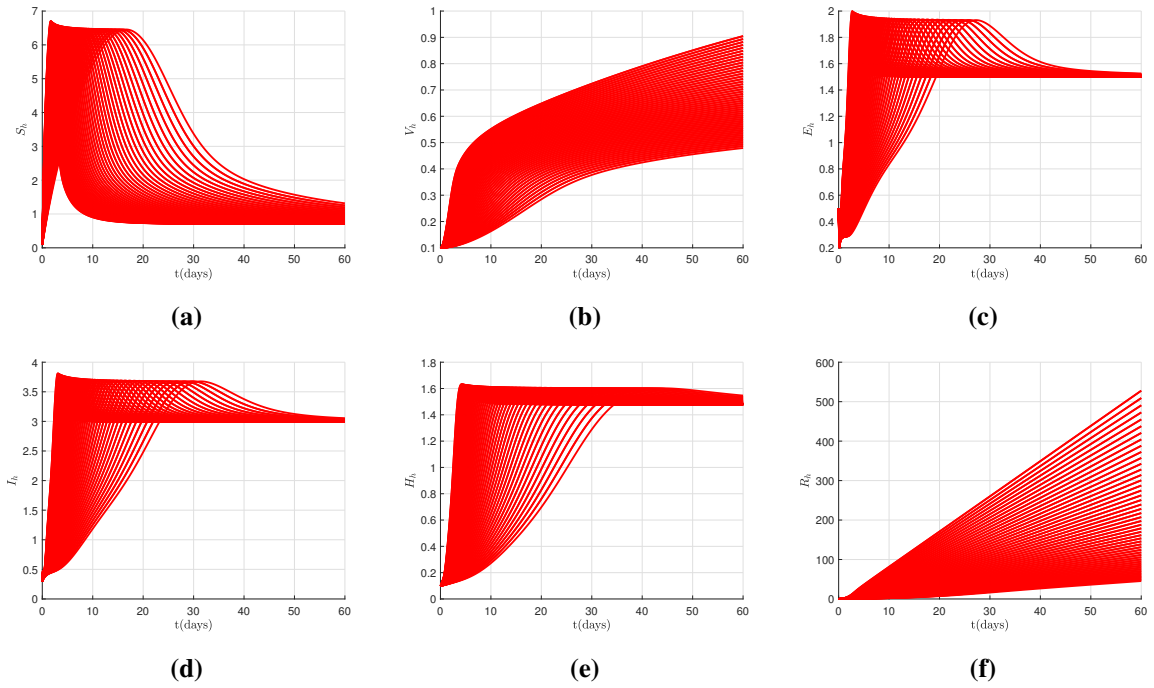

Figure 10. Dynamics of the S_h, V_h, E_h, I_h, H_h, and R_h compartments over time for different fractional orders ζ.

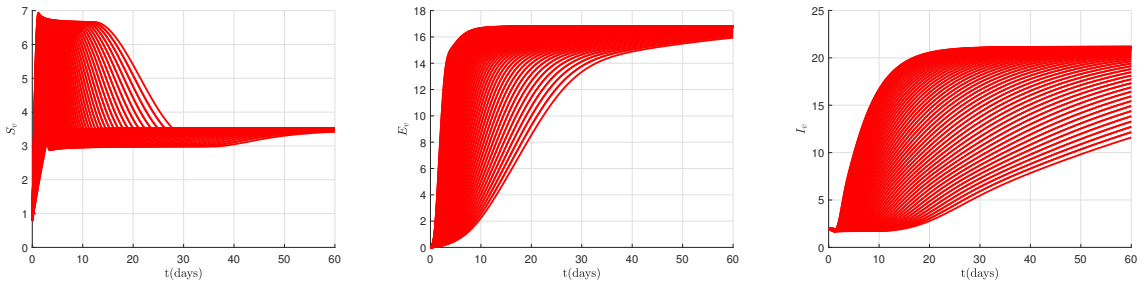

(a) **(b)** **(c)**

Figure 11. Dynamics of S_v, E_v, I_v compartments over time for different fractional orders ζ.

In contrast, Figures 12–20, the 3D and contour plots of S_h, V_h, E_h, I_h, H_h, R_h, S_v, E_v, and I_v illustrate the combined influence of time and the fractional order $\zeta \in [0.1, 0.99]$ for the human and vector populations. Consequently, lower values of ζ produce smoother and slower transitions, indicating strong memory effects, while larger values of ζ recover faster dynamics consistent with the classical integer-order model.

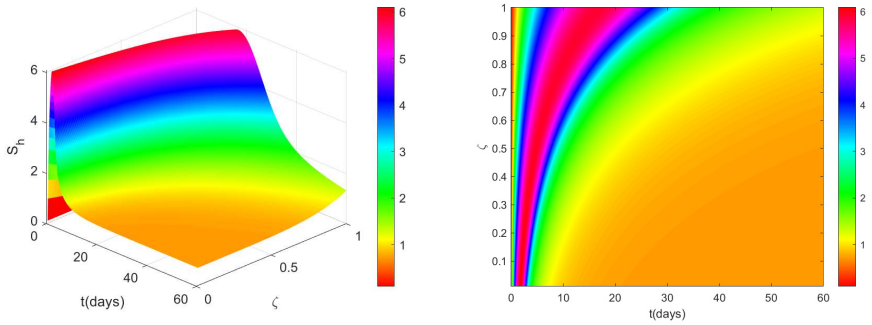

(a) **(b)**

Figure 12. 3D surface and contour plots illustrate the dynamics of S_h over time and fractional order $\zeta \in [0.1, 0.99]$.

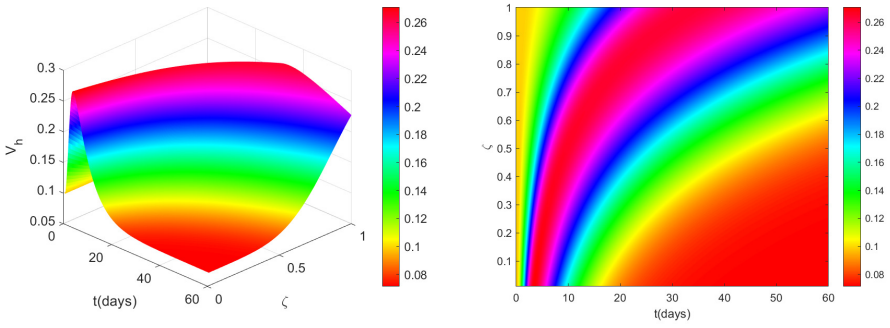

(a) **(b)**

Figure 13. 3D surface and contour plots illustrate the dynamics of V_h over time and fractional order $\zeta \in [0.1, 0.99]$.

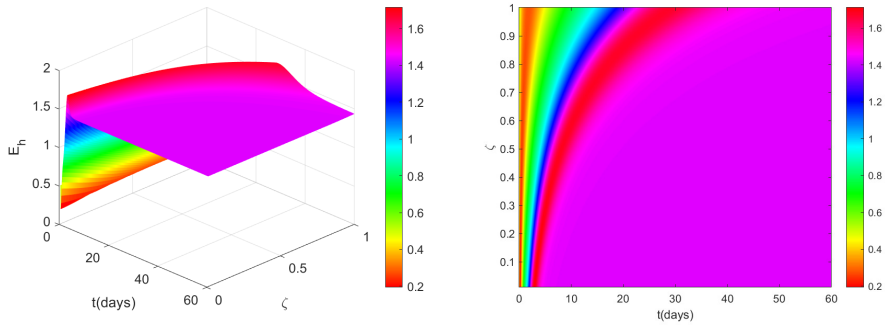

(a) **(b)**

Figure 14. 3D surface and contour plots illustrate the dynamics of E_h over time and fractional order $\zeta \in [0.1, 0.99]$.

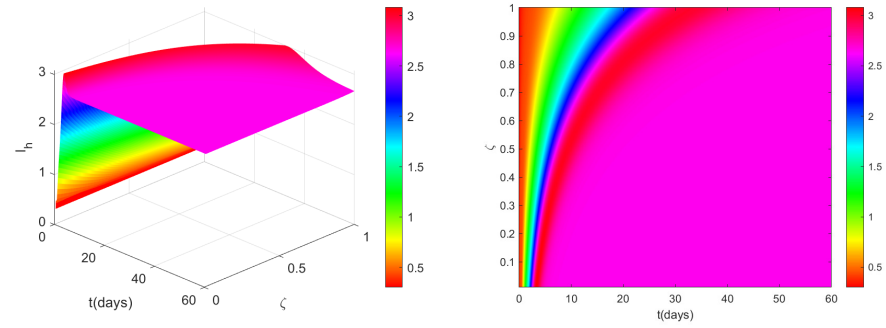

(a) **(b)**

Figure 15. 3D surface and contour plots illustrate the dynamics of I_h over time and fractional order $\zeta \in [0.1, 0.99]$.

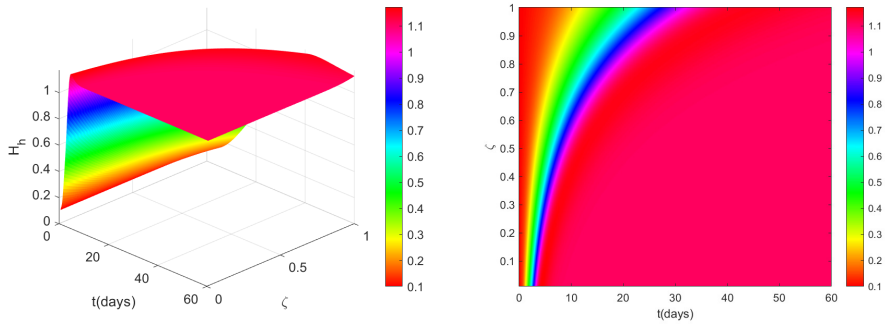

(a) **(b)**

Figure 16. 3D surface and contour plots illustrate the dynamics of H_h over time and fractional order $\zeta \in [0.1, 0.99]$.

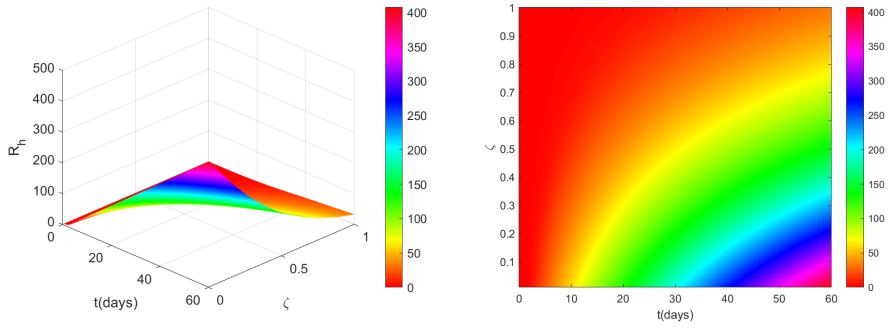

(a) **(b)**

Figure 17. 3D surface and contour plots illustrate the dynamics of R_h over time and fractional order $\zeta \in [0.1, 0.99]$.

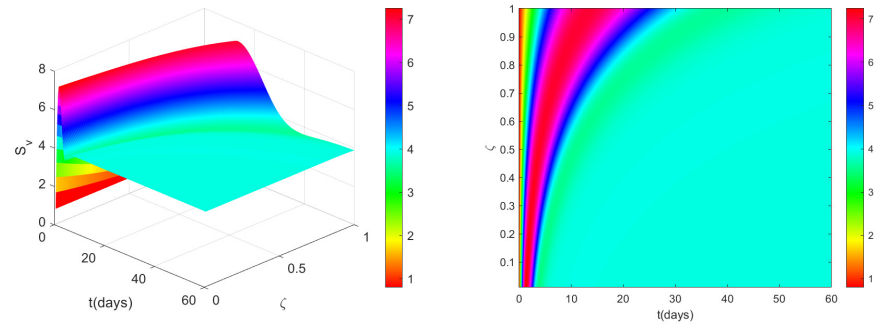

(a) **(b)**

Figure 18. 3D surface and contour plots illustrate the dynamics of S_v over time and fractional order $\zeta \in [0.1, 0.99]$.

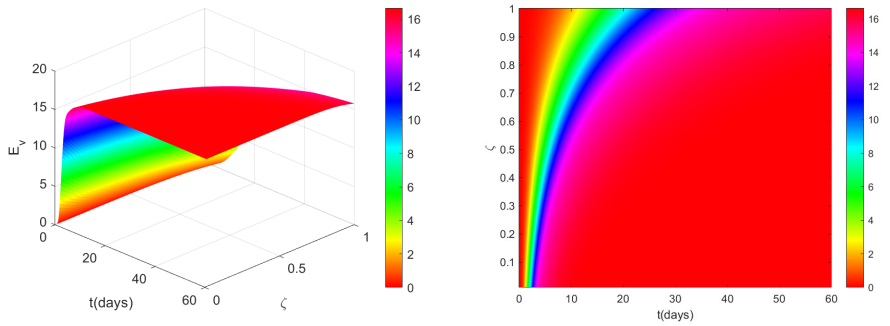

(a) **(b)**

Figure 19. 3D surface and contour plots illustrate the dynamics of E_v over time and fractional order $\zeta \in [0.1, 0.99]$.

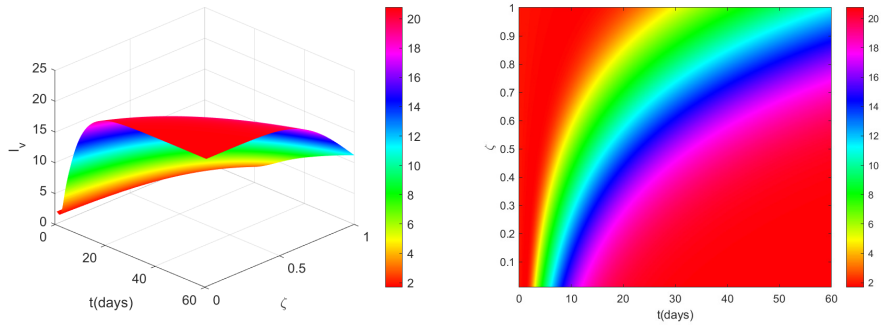

(a) **(b)**

Figure 20. 3D surface and contour plots illustrate the dynamics of I_v over time and fractional order $\zeta \in [0.1, 0.99]$.

Furthermore, we examine the influence of key parameters in the fractional-order model, as shown in Figure 21, by increasing the vaccination rate ν from 0.01 to 0.09, which leads to a reduction in the susceptible, exposed, infectious, and hospitalized human populations, while the vaccinated class increases. This behavior highlights the effectiveness of vaccination in controlling disease transmission and enhancing the recovered population. Figure 22 shows that decreasing the biting rate a leads to a slower depletion of the susceptible human population and a noticeable reduction in the exposed and infectious human classes. Similarly, reduced biting lowers transmission from humans to vectors, resulting in declines in the exposed and infectious vector populations. These results emphasize that reducing vector biting effectively suppresses the spread of TBE in both human and vector populations.

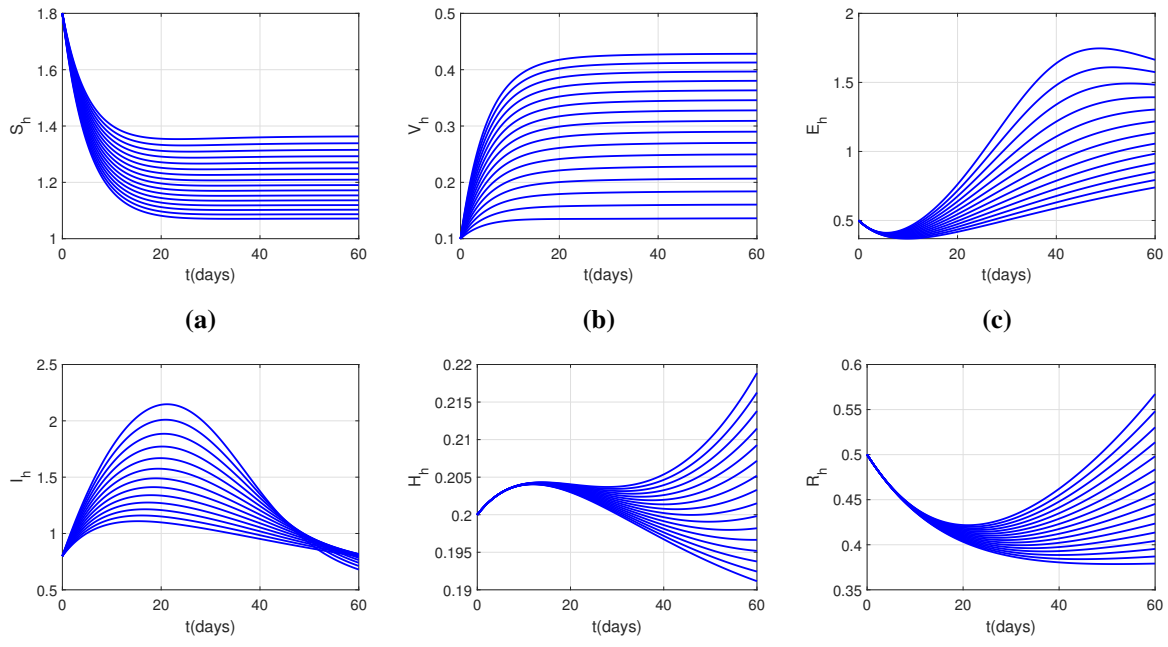

(a) **(b)** **(c)**

(d) **(e)** **(f)**

Figure 21. Effect of the vaccination rate ν on the human population classes, while the fractional order is fixed at $\zeta = 0.98$.

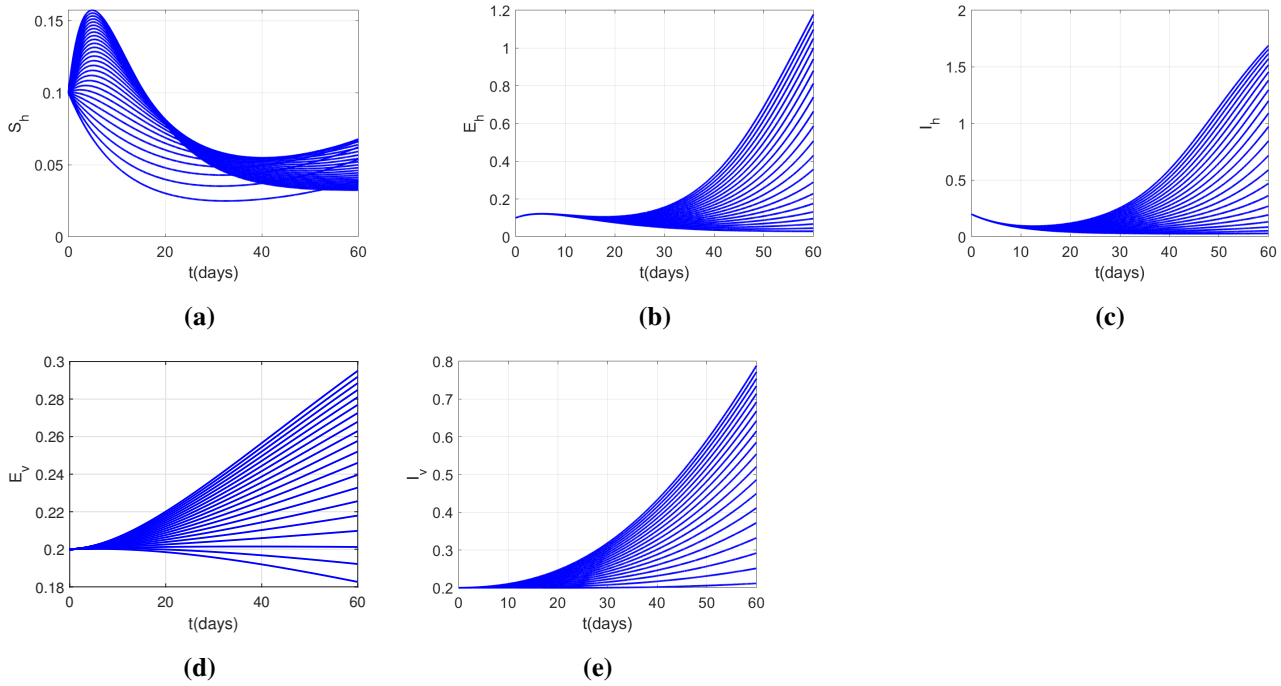

Figure 22. Impact of the biting rate a on the human and vector population, while the fractional order is fixed at $\zeta = 0.98$.

10. Conclusions

In this study, we developed and analyzed a fractional-order mathematical model to describe the transmission dynamics of TBE in human and vector populations. Model parameters were estimated using a nonlinear least-squares approach based on reported TBE case data. Consistent with this finding, the fractional-order model achieved a noticeably improved fit to the observed data compared with its integer-order counterpart, as confirmed by a low root mean square error. We confirmed that the endemic equilibrium achieves global asymptotic stability when $\mathcal{R}_0 > 1$, while the disease-free equilibrium is locally asymptotically stable when $\mathcal{R}_0 < 1$. Furthermore, we conducted a sensitivity analysis to identify the critical parameters influencing $\mathcal{R}_0$. The fractional order $\zeta = 0.71$ indicates the presence of significant memory effects in TBE transmission dynamics. Moreover, using the Adams-Moulton numerical approach, we carried out numerical simulations supported by contour and three-dimensional surface visualizations, demonstrating that variations in key epidemiological parameters can substantially reduce infection levels in humans and vectors. In particular, increasing the vaccination rate was shown to have a pronounced impact on suppressing disease transmission. The proposed fractional-order framework offers a robust and data-consistent tool for understanding TBE dynamics and evaluating control strategies. These results show the importance of incorporating memory effects of mathematical modeling of TBE and provide valuable insights for the evaluation of strategies aimed at reducing disease transmission, particularly vaccination-based interventions. Taken together, these findings provide significant guidance to develop focused and effective public health interventions aimed at epidemic containment. In future work may extend this framework by

incorporating optimal control formulations to assess cost effective prevention and treatment strategies under memory dependent transmission dynamics.

Use of AI tools declaration

The authors declare that they have not used Artificial Intelligence (AI) tools in the creation of this article.

Acknowledgments

The authors would like to thank Prince Sultan University for APC and support through the TAS research lab.

Conflict of interest

The authors declare there is no conflicts of interest.

Author contributions

Writing-original draft: S.U., Z.U.; A Formal analysis: S.U., T.A., Z.U.; Investigation: S.U., Z.U.; Project administration: M.M.K.; Resources: M.M.K., K.S., T.A.; Software: Z.U.; Supervision: T.A.; Writing-review & editing: S.K., Z.U., M.M.K., K.S., T.A.

References

1. L. Lindquist, O. Vapalahti, Tick-borne encephalitis, *Lancet*, **371** (2008), 1861–1871. https://doi.org/10.1016/S0140-6736(08)60800-4
2. M. Holding, S. Dowall, R. Hewson, Detection of tick-borne encephalitis virus in the UK, *Lancet*, **395** (2020), 411. https://doi.org/10.1016/S0140-6736(20)30040-4
3. T. Füzik, P. Formanová, D. Ruzek, K. Yoshii, M. Niedrig, P. Plevka, Structure of tick-borne encephalitis virus and its neutralization by a monoclonal antibody, *Nat. Commun.*, **9** (2018), 436. https://doi.org/10.1038/s41467-018-02882-0
4. P. J. Hotez, M. E. Bottazzi, U. Strych, L. Y. Chang, Y. A. L. Lim, M. M. Goodenow, et al. Neglected tropical diseases among the Association of Southeast Asian Nations (ASEAN): Overview and Update, *PLoS Negl Trop Dis.*, **9** (2015), e0003575. https://doi.org/10.1371/journal.pntd.0003575
5. J. Süss, Epidemiology and ecology of TBE relevant to the production of effective vaccines, *Vaccine*, **21** (2003), S19–S35. https://doi.org/10.1016/S0264-410X(02)00812-5
6. WHO Publication, Vaccines against tick-borne encephalitis: WHO position paper Recommendations, *Vaccine*, **29** (2011), 8769–8770. https://doi.org/10.1016/j.vaccine.2011.07.024

7. Y. Xing, H. J. Schmitt, A. G. Arguedas, J. Yang, Tick-borne encephalitis in China: A review of epidemiology and vaccines, *Vaccine* **35** (2017), 1227–1237. https://doi.org/10.1016/j.vaccine.2017.01.015
8. J. Beauté, G. Spiteri, E. Warns-Petit, H. Zeller, Tick-borne encephalitis in Europe, 2012 to 2016, *Eurosurveillance* **23** (2018), 1800201. https://doi.org/10.2807/1560-7917.ES.2018.23.45.1800201
9. S. Jahfari, A. de Vries, J. M. Rijks, S. Van Gucht, H. Vennema, H. Sprong, et al. Tick-borne encephalitis virus in ticks and Roe Deer, the Netherlands, *Emerg. Infect. Dis.*, **23** (2017), 1028–1030. https://doi.org/10.3201/eid2306.161247
10. K. L. Mansfield, L. Jizhou, L. P. Phipps, N. Johnson, Emerging tick-borne viruses in the twenty-first century, *Front. Cell. Infect. Microbiol.*, **7** (2017), 298. https://doi.org/10.3389/fcimb.2017.00298
11. H. Qin, X. Xin, Q. Tang, X. Feng, B. Yin, The prevalence of tick-borne encephalitis virus in the ticks and humans of China from 2000 to 2023: A systematic review and meta-analysis, *Vet. Sci*., **12** (2025), 146. https://doi.org/10.3390/vetsci12020146
12. R. X. Sun, S. J. Lai, Y. Yang, X. L. Li, K. Liu, H. W. Yao, et al., Mapping the distribution of tick-borne encephalitis in mainland China, *Ticks Tick Borne Dis.*, **8** (2017), 631–639. https://doi.org/10.1016/j.ttbdis.2017.04.009
13. M. Kwasnik, J. Rola, W. Rozek, Tick-borne encephalitis—Review of the current status, *J. Clin. Med.*, **12** (2023), 6603. https://doi.org/10.3390/jcm12206603
14. W. Miazga, K. Wnuk, T. Tatara, J. Aswitalski, A. Matera, U. Religioni, et al., The long-term efficacy of tick-borne encephalitis vaccines available in Europe—A systematic review, *BMC Infect. Dis.*, **23** (2023), 621. https://doi.org/10.1186/s12879-023-08562-9
15. Zakirullah, Measles disease spread and control via vaccination and treatment: A mathematical framework, *Chaos Solitons Fractals*, **203** (2026), 117703. https://doi.org/10.1016/j.chaos.2025.117703
16. Zakirullah, A mathematical model of pneumococcal pneumonia infection dynamics using treatment and vaccination interventions, *Int. J. Appl. Comput. Math.*, **11** (2025), 112. https://doi.org/10.1007/s40819-025-01928-4
17. H. Kollaritsch, M. Paulke-Korinek, H. Holzmann, J. Hombach, B. Bjorvatn, A. Barrett, Vaccines and vaccination against tick-borne encephalitis, *Expert Rev. Vaccines*, **11** (2012), 1103–1119. https://doi.org/10.1586/erv.12.86
18. M. Du, Z. Wang, H. Hu, Measuring memory with the order of fractional derivative, *Sci. Rep.*, **3** (2013), 3431. https://doi.org/10.1038/srep03431
19. P. A. Naik, B. M. Yeolekar, S. Qureshi, M. Yavuz, Z. Huang, M. Yeolekar, Fractional insights in tumor modeling: An interactive study between tumor carcinogenesis and macrophage activation, *Adv. Theory Simul.*, **8** (2025), 2401477. https://doi.org/10.1002/adts.202401477
20. H. Khan, J. Alzabut, D. K. Almutairi, W. K. Alqurashi, The use of artificial intelligence in data analysis with error recognitions in liver transplantation in HIV-AIDs patients using modified abc fractional order operators, *Fractal Fract.*, **9** (2025), 16. https://doi.org/10.3390/fractalfract9010016

21. A. S. Devi, P. A. Naik, S. Boulaaras, N. Sene, Z. Huang, Understanding the transmission mechanism of HIV/TB Co-infection using fractional framework with optimal control, *Int. J. Num. Model.*, **38** (2025), e70097. https://doi.org/10.1002/jnm.70097
22. A. Akgül, S. Ahmad, A. Ullah, D. Baleanu, E. K. Akgül, A novel method for analysing the fractal fractional integrator circuit, *Alexandria Eng. J.*, **60** (2021), 3721–3729. https://doi.org/10.1016/j.aej.2021.01.061
23. L. Xuan, S. Ahmad, A. Ullah, S. Saifullah, A. Akgül, H. Qu, Bifurcations, stability analysis and complex dynamics of Caputo fractal-fractional cancer model, *Chaos Solitons Fractals*, **159** (2022), 112113. https://doi.org/10.1016/j.chaos.2022.112113
24. Zakirullah, C. Lu, L. Li, K. Shah, B. Abdalla, T. Abdeljawad, Mathematical insights into chaos in fractional-order fishery model, *Model. Earth. Syst. Environ.*, **11** (2025), 201. https://doi.org/10.1007/s40808-025-02375-2
25. P. A. Naik, B. M. Yeolekar, S. Qureshi, M. Yeolekar, A. Madzvamuse, Modeling and analysis of the fractional-order epidemic model to investigate mutual influence in HIV/HCV co-infection, *Nonlinear Dyn.*, **112** (2024), 11679–11710. https://doi.org/10.1007/s11071-024-09653-1
26. A. Alkhazzan, J. Wang, Y. Nie, S. M. A. Shah, D. K. Almutairi, H. Khan, et al., Lyapunov-based analysis and worm extinction in wireless networks using stochastic SVEIR model, *Alexandria Eng. J*, **118** (2025), 337–353. https://doi.org/10.1016/j.aej.2025.01.040
27. H. Khan, W. F. Alfwzan, J. Alzabut, D. K. Almutairi, M. A. Azim, R. Thinakaran, Artificial intelligence and neural networking for an analysis of fractal-fractional Zika virus model, *Fractals*, **33** (2025), 2540143. https://doi.org/10.1142/S0218348X25401437
28. A. Ahmad, M. Farman, P. A. Naik, E. Hincal, F. Iqbal, Z. Huang, Bifurcation and theoretical analysis of a fractional-order hepatitis B epidemic model incorporating different chronic stages of infection, *J. Appl. Math. Comput.*, **71** (2025), 1543–1564. https://doi.org/10.1007/s12190-024-02301-2
29. P. A. Naik, M. Farman, K. Jamil, K. S. Nisar, M. A. Hashmi, Z. Huang, Modeling and analysis using piecewise hybrid fractional operator in time scale measure for Ebola virus epidemics under Mittag–Leffler kernel, *Sci. Rep.*, **14** (2024), 24963. https://doi.org/10.1038/s41598-024-75644-2
30. E. Pustijanac, M. Bursi, J. Talapko, I. Skrlec, T. Mestrovi, D. Lisnjic, Tick-borne encephalitis virus: A comprehensive review of transmission, pathogenesis, epidemiology, clinical manifestations, diagnosis, and prevention, *Microorganisms*, **11** (2023), 1634. https://doi.org/10.3390/microorganisms11071634
31. K. L. Mansfield, N. Johnson, L. P. Phipps, J. R. Stephenson, A. R. Fooks, T. Solomon, Tick-borne encephalitis virus—A review of an emerging zoonosis, *J. Gen. Virol.*, **90** (2009), 1781–1794. https://doi.org/10.1099/vir.0.011437-0
32. World Health Organization, Tick-borne encephalitis, 2025. Available from: https://www.who.int/health-topics/tick-borne-encephalitis.
33. R. M. Vorou, V. G. Papavassiliou, S. Tsiodras, Emerging zoonoses and vector-borne infections affecting humans in Europe, *Epidemiol. Infect.*, **135** (2007), 1231–1247. https://doi.org/10.1017/S0950268807008527

34. R. Kaiser, J. J. Archelos-Garcia, W. Jilg, S. Rauer, M. Sturzenegger, Tick-borne encephalitis (TBE), *Neurol. Int. Open*, **01** (2017), E48–E55. https://doi.org/10.1055/s-0043-103258
35. V. Mittova, Z. R. Tsetskhladze, C. Motsonelidze, R. Palumbo, C. Vicidomini, G. N. Roviello, Tick-borne encephalitis virus (TBEV): Epidemiology, diagnosis, therapeutic approaches and some molecular aspects an updated review, *Microbiol. Res.*, **15** (2024), 2619–2649. https://doi.org/10.3390/microbiolres15040174 .
36. J. Süss, Tick-borne encephalitis 2010: Epidemiology, risk areas, and virus strains in Europe and Asia—An overview, *Ticks Tick Borne Dis.* **2** (2011), 2–15. https://doi.org/10.1016/j.ttbdis.2010.10.007
37. I, Podlubny, *Fractional Differential Equations*, Academic Press, New York, 1998. Available from: https://www.elsevier.com/books/fractional-differential-equations/podlubny/978-0-12-558840-9.
38. Y, Povstenko, Linear Fractional Diffusion-Wave Equation for Scientists and Engineers, Birkhauser Cham. Available from: https://doi.org/10.1007/978-3-319-17954-4.
39. A. A. Kilbas, H. M. Srivastava, J. J. Trujillo, *Theory and Applications of Fractional Differential Equations*, Elsevier: Amsterdam, The Netherlands, 2006. Available from: https://www.sciencedirect.com/bookseries/north-holland-mathematics-studies/vol/204.
40. Y. Zhu, T. Jiang, Z. Sun, J. Yin, H. Zhao, X. Zhou, K. Kassegne, Tick-borne infectious diseases in China, 2003–2023, *China CDC Weekly*, **7** (2025), 900. https://doi.org/10.46234/ccdcw2025.150
41. China Population (LIVE), *Worldometer*, 2025. Available from: https://www.worldometers.info/world-population/china-population/.
42. National Bureau of Statistics of China, Statistical communiqué of the People's Republic of China on the 2025 national economic and social development, 2026. Available from: https://www.stats.gov.cn/english/PressRelease/202602/t20260228_1962661.html.
43. X. O'Neill, A. White, C. Gortízar, F. Ruiz-Fons, The impact of host abundance on the epidemiology of tick-borne infection, *Bull. Math. Biol.*, **85** (2023), 30. https://doi.org/10.1007/s11538-023-01133-8
44. C. Li, C. Tao, On the fractional Adams method, *Comput. Math. Appl.*, **58** (2009), 1573–1588. https://doi.org/10.1016/j.camwa.2009.07.050

AIMS Press